rLSTM-AE for dimension reduction and its application to active learning-based dynamic reliability analysis

Yu Zhang[a], You Dong[a,*], Michael Beer[b,c,d]

[a]Department of Civil and Environmental Engineering, The Hong Kong Polytechnic University, Hong Kong, China
[b]Institute for Risk and Reliability, Leibniz University Hannover, Callinstr. 34, Hannover 30167, Germany
[c]Institute for Risk and Uncertainty, University of Liverpool, Peach Street, Liverpool L69 7ZF, United Kingdom
[d]School of Civil Engineering, Tsinghua University, Beijing, China

Abstract

A novel method termed rLSTM-AE is developed for the low-dimensional latent space identification of the stochastic dynamic systems with more than 1000 input random variables and the active learning-based dynamic reliability analysis. First, the long short-term memory network considers both the time-variant stochastic excitation and the time-invariant random variables is developed (rLSTM), which adopts the time-series excitation as the pertinent input feature and makes it available for the metamodeling of the high-dimensional stochastic dynamic systems. To circumvent the insufficient accuracy of deep neural networks for reliability analysis results from the limited observations, autoencoder (AE) is incorporated with the rLSTM (rLSTM-AE) and utilized to decompose the approximate extreme value space found by rLSTM onto a low-dimensional latent space. The dimension of the latent space is adaptively determined by a Gaussian process regression reconstruction error, which enables the Gaussian process regression with the similar accuracy as rLSTM regarding the extreme responses prediction. The proposed rLSTM-AE conducts the low-dimensional features extraction from the perspective of the output space decomposition and considers the time-dependent property of the dynamic systems. Finally, the detected latent variables can be combined with the active learning-based Gaussian process regression for the high-dimensional dynamic reliability analysis. One single-degree-of-freedom system and a reinforced concrete frame structure subjected to the stochastic excitation are investigated to validate the performance of the proposed method.

Keywords: High dimension, stochastic dynamic system, metamodel, latent space, reliability analysis

1. Introduction

Uncertainties are inevitable and widely exist in initial conditions, boundary conditions, constitutive laws and etc., which significantly affect the performance of engineering systems. Therefore, it is of paramount importance to quantify the effect of these uncertainties on the response of interest. However, uncertainty propagation remains a challenging task sine the computer codes for simulating the practical engineering systems require significant computational power, which makes the direct approaches such as Monte Carlo simulation unavailable. Recently, metamodel or surrogate model techniques have gained increasing popularity for uncertainty propagation [1–3]. Metamodels are constructed by consuming limited simulation-based data and the trained surrogate model can be subsequently utilized to replace the original computationally expensive real model for uncertainty propagation tasks.

Commonly used metamodels include the polynomial chaos expansion (PCE) [4–7], Gaussian process regression (GPR) (or Kriging model) [8–10], and support vector regression [11–13]. However, these surrogate models usually suffer from the so called "curse of dimensionality". For instance, the number of unknown coefficients of PCE terms increases dramatically with the dimension of inputs when the regression method is employed, which means

*Corresponding author
Email addresses: yuphd.zhang@connect.polyu.hk (Yu Zhang), you.dong@polyu.edu.hk (You Dong), beer@irz.uni-hannover.de (Michael Beer)

that a substantial number of training samples are required to accurately determine the coefficients. To mitigate this issue, an adaptive algorithm that can identify the important terms was developed to build the sparse PCE [1]. Dimension-reduction model based on sensitivity analysis was combined with PCE to reduce the number of training samples [14]. Researchers also explored the PCE with the partial least square for high-dimensional uncertainty propagation problems [15, 16]. However, these works seldom place emphases on the high-dimensional stochastic dynamic systems. GPR has been widely employed for the active learning-based reliability analysis in recent years due to the elegant stochastic property of Gaussian process, that is, apart from providing a mean prediction, the uncertainty of the prediction can be quantified by the GPR model. Echard et al. developed an active learning-based Kriging model with MCS, which can adaptively enrich the training set with samples that can significantly improve the accuracy of Kriging model [2]. Then, this active learning-based approach has been further developed in terms of the sampling methods [17–20], learning functions [21–23] and stopping criteria [24–26]. Nevertheless, these active learning-based approaches are not applicable to high-dimensional problems due to the curse of dimensioality, let alone the stochastic dynamic systems with more then 1000 input features investigated in this paper.

Stochastic dynamic systems consider uncertainties both from structural parameters and the external excitation, which are common in engineering problems. For instance, structures subjected to the fully non-stationary seismic ground motions. Non-stationary stochastic processes are utilized to reflect the natural randomness and simulate the excitation. Various approaches can be employed such as the spectral representation [27–30], Karhunen-Loeve (K-L) expansion [5, 31] and etc.. Generally, a considerable number of random variables (usually 500$\sim$1000) is required to sufficiently describe the features of the stochastic process, which leads to a high-dimensional uncertainty propagation problem. In this paper, stochastic dynamic systems with more than 1000 input random variables are investigated. Metamodel is not suitable for dealing with this problem since it significantly suffers from the curse of dimensionality and the time-dependent complex dynamics involved. To tackle this issue, Chen and Li focused on the extreme responses and the probability density evolution method was employed to yield the extreme value distribution [32]. Then the first-passage failure probability can be readily obtained from the extreme value distribution. The high-dimensional problem can be also circumvented from the perspective of moment-based methods, which can cover an unknown extreme value distribution by fitting a series of statistical moments estimated by sampling techniques [33–35]. However, it is hard to select a suitable distribution model to fit the extreme value distribution and ensure the accuracy of the statistical moments estimation.

To build metamodel for the high-dimensional systems, a fundamental idea is to find a low-dimensional representation of the original high-dimensional space. Dimension-reduction techniques such as the sliced inverse regression and active subspace have been utilized for building surrogate models and reliability analysis [36–38]. However, these linear methods may have limitations in representing complex data [39]. The kernel principle component analysis [40] and the deep neural networks-based feature extraction method termed autoencoder [41] were also explored for high-dimensional reliability analysis [42, 43]. Regarding the metamodeling for the dynamical systems, Spiridonakos and Chatzi [44] developed a metamodeling strategy for nonlinear dynamical systems by using the PCE and the nonlinear autoregressive with exogenous input model (NARX). Then, a similar Kriging-NARX model was proposed [45]. Recently, a mNARX surrogate model has been proposed for approximating the response of complex dynamical systems [46]. Inspired by the reduced order technique, the proper orthogonal decomposition was combined with the Kriging model for the uncertainty propagation of dynamical systems [47]. Yang and Perdikaris developed a conditional deep surrogate model for stochastic, high-dimensional dynamic systems [48]. A feature mapping strategy was proposed to build the surrogate model of nonlinear stochastic dynamic systems and a 100-dimensional system was studied [49]. Soize and Ghanem [50] recently developed a probabilistic-learning-based stochastic surrogate model for nonlinear dynamical systems. However, the approach to dealing with the high-dimensional random phases in simulating the stochastic excitation should be further investigated. Simultaneously, it is essential to consider both the time-variant stochastic excitation and time-invariant random structural parameters. Although Zhou and Peng investigated the reliability analysis of a 110-dimensional stochastic dynamic system by combining the autoencoder and GPR [39], a simplified method for simulating the stochastic ground motions termed the stochastic harmonic function representation method [51] was employed. Moreover, only the extreme responses were considered in Ref. [39] when constructing the surrogate model and the time history responses were ignored.

Therefore, the high-dimensional stochastic dynamic systems with more than 1000 input features have not been studied in terms of the metamodel construction for the time history responses prediction and the high-dimensional reliability analysis. Note that the high-dimensional problem is primarily caused by the thousands of random phases for simulating the stochastic process. In fact, these random variables are not pertinent input features but the generated time-variant stochastic excitations are. A powerful deep learning tool called the long short-term memory (LSTM) can be employed to deal with the sequence-to-sequence data so that the high-dimensional random phases can be circumvented. The LSTM has been investigated for metamodeling of nonlinear structures [52, 53] and only the time-variant excitation serves as the input feature. However, the uncertainties of structural parameters and seismic ground motions are not considered for the metamodel construction. In this paper, a LSTM network termed rLSTM considering both the time-invariant random structural parameters and the time-variant stochastic excitation is developed for high-dimensional metamodel construction by data concatenation and normalization. The high-dimensional reliability analysis of the stochastic dynamic systems is of concern. It is always hard to build a metamodel across the whole domain of the stochastic dynamic systems with limited observations. Therefore, the accuracy of the rLSTM may be not sufficient for reliability analysis problems due to the limited observations. To address this issue, a novel latent space detection method termed the rLSTM-AE is developed with the aid of the constructed rLSTM, where "AE" denotes the autoencoder. Autoencoder here is utilized to decompose the one-dimensional approximate extreme value space predicted by rLSTM onto a low-dimensional latent space and the best dimension is adaptively determined by minimizing the GPR reconstruction error. rLSTM-AE brings insights of the latent variables extraction for high-dimensional stochastic dynamic systems from the perspective of the output space. Moreover, the time-dependent property of the dynamic systems is considered during the dimension-reduction process. Finally, the detected latent variables can be combined with the active learning-based GPR model for the high-dimensional dynamic reliability analysis. This paper is organized as the follows. Section 2 presents the proposed rLSTM network for metamodeling of the high-dimensional stochastic dynamic systems. The paradigm of the novel latent space detection method and its application to the active learning-based reliability analysis are introduced in Section 3. Two high-dimensional stochastic dynamic systems with more than 1000 input random variables are investigated in Section 4 to validate the accuracy and efficiency of the proposed method.

2. The proposed rLSTM for metamodeling of the high-dimensional stochastic dynamic systems

2.1. A typical stochastic dynamic system: structures subjected to the stochastic seismic excitation

The governing equation for a multi-degree-of-freedom system subjected to the stochastic seismic excitation can be given by:

$$\mathbf{M}\left(\mathbf{X}_S\right)\ddot{\mathbf{u}} + \mathbf{C}\dot{\mathbf{u}} + \mathbf{K}\left(\mathbf{X}_S\right)\mathbf{u} + \mathbf{F} = -\mathbf{M}\left(\mathbf{X}_S\right)\mathbf{I}a\left(\mathbf{X}_E, t\right) \tag{1}$$

where $\mathbf{M}$, $\mathbf{C}$ and $\mathbf{K}$ are the mass, damping and stiffness matrix, respectively; $\ddot{\mathbf{u}}$, $\dot{\mathbf{u}}$ and $\mathbf{u}$ are acceleration, velocity and displacement vector, respectively; $\mathbf{F}$ denotes the restoring force vector and $\mathbf{I}$ is the force distribution vector; $a\left(\mathbf{X}_E, t\right)$ represents the non-stationary stochastic seismic ground motions. $\mathbf{X}_E = \left(X_{E1}, X_{E2}, ..., X_{Ed_1}\right)$ includes d_1 random variables accounting for uncertainties in seismic ground motions. $\mathbf{X}_S = \left(X_{S1}, X_{S2}, ..., X_{Sd_2}\right)$ is a random vector containing d_2 random variables related to the structural parameters.

Various approaches have been developed for generating the stochastic seismic excitation [30, 31, 54]. Herein, the spectral representation method is adopted [54]:

$$a\left(t\right) = \sqrt{2}\sum_{k=0}^{d_1-1}\sqrt{2S_a\left(w_k, t\right)\Delta w}\left[w_k t + \phi_k\right] \tag{2}$$

where $S_a\left(w, t\right)$ is the double-sided evolutionary power spectral density function of the frequency w and time t:

$$S_a\left(w, t\right) = \left|f\left(w, t\right)\right|^2 S\left(w\right) \tag{3}$$

in which $f\left(w, t\right)$ is the amplitude envelope function defined by:

$$f\left(w, t\right) = \left[\frac{t}{5}\exp\left(1 - \frac{t}{5}\right)\right]^2 \tag{4}$$

and $S\left(w\right)$ is the one-sided power spectral density function defined by Clough-Penzien spectrum [33]:

$$S\left(w\right)=\frac{w_{\mathrm{g}}^{4}+4\zeta_{\mathrm{g}}^{2}w_{\mathrm{g}}^{2}w^{2}}{\left(w^{2}-w_{\mathrm{g}}^{2}\right)^{2}+4\zeta_{\mathrm{g}}^{2}w_{\mathrm{g}}^{2}w^{2}}\cdot\frac{w^{4}}{\left(w^{2}-w_{f}^{2}\right)^{2}+4\zeta_{f}^{2}w_{f}^{2}w^{2}}S_{0} \tag{5}$$

in which S_0 is the spectral intensity of seismic acceleration processes; w_g and ζ_g are the dominant frequency and damping ratio of the site soil, respectively; w_f and ζ_f are the parameters of the second filter mainly hindering the low-frequency component of seismic acceleration [54]. The discrete frequency w_i gives:

$$w_k = k\Delta w,\ k = 0, 1, ..., d_1 - 1 \tag{6}$$

where Δw is the frequency interval. In this paper, these parameters are specified as: $w_{\mathrm{g}} = 5\pi$ rad/s, $w_f = 0.1w_{\mathrm{g}}$ rad/s, $\zeta_{\mathrm{g}} = \zeta_f = 0.60$, $S_0 = 48.9332\ \mathrm{cm}^2/\mathrm{s}^3$, $\Delta = 0.1\mathrm{rad}/s$, $d_1 = 1001$ and t is a time sequence ranging from 0 to 20s with a interval of 0.02s. Hence, the phase angles ϕ_ks are 1001 independent uniformly distributed random variables over $[0, 2\pi]$, which leads to a high-dimensional stochastic dynamic system. Constructing metamodel and conducting reliability analysis for the high-dimensional stochastic dynamic system are challenging due to the curse of dimensionality and complex dynamics.

2.2. Long short-term memory considering both time-variant and time-invariant features: rLSTM

The primary reason for the high-dimensional problem in stochastic dynamic systems is the inclusion of a large number of random variables for generating the stochastic excitation. Hence, if these random variables are treated as input features for a stochastic dynamic system, conducting metamodeling or reliability analysis would be tricky. However, these random variables have little effect on the response of interest since the dominant feature is the excitation generated by them. Therefore, if the time-series excitation is employed as the input feature directly when building metamodel, the high-dimensional problem can be circumvented. Long short-term memory network is a powerful deep

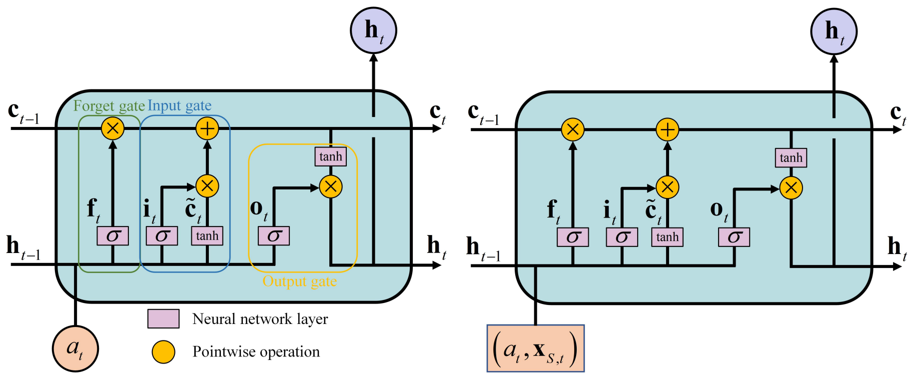

(a) LSTM cell (b) rLSTM cell

Figure 1: LSTM and rLSTM cells

learning tool to deal with the sequence-to-sequence data and has shown its advantages on capturing the time-series input-output relationship [52, 53]. A common LSTM unit is composed of a cell c, a forget gate f, an input gate i and an output gate o, which are shown in Fig. 1 (a). The cell memorizes the state at the previous time step to capture the long-term dependency and three gates control the information into and out of the cell. The forget gate decides what information can be thrown away, the input gate determines the new information that can be stored in the current state and the output gate decides what information to output according to the previous and current states. At time step t, the equations for the forward process of a LSTM cell can be given by:

$$
\begin{aligned}
&\mathbf{i}_t = \sigma\left(\mathbf{W}_{ai} a_t + \mathbf{W}_{hi} \mathbf{h}_{t-1} + \mathbf{b}_i\right) \\
&\tilde{\mathbf{c}}_t = \tanh\left(\mathbf{W}_{ac} a_t + \mathbf{W}_{hc} \mathbf{h}_{t-1} + \mathbf{b}_c\right) \\
&\mathbf{o}_t = \sigma\left(\mathbf{W}_{ao} a_t + \mathbf{W}_{ho} \mathbf{h}_{t-1} + \mathbf{b}_o\right) \\
&\mathbf{c}_t = \mathbf{f}_t \odot \mathbf{c}_{t-1} + \mathbf{i}_t \odot \tilde{\mathbf{c}}_t \\
&\mathbf{h}_t = \mathbf{o}_t \odot \tanh\left(\mathbf{c}_t\right)
\end{aligned}
\tag{7}
$$

where $\mathbf{W}$ and $\mathbf{b}$ are the weight matrices and bias vectors, respectively, $\mathbf{h}$ represents the hidden state and a_t denotes the input feature (seismic ground motions in this paper) at time step t. The notation $\odot$ represents Hadamard product (element-wise product). σ and "tanh" represent the sigmoid and hyperbolic tangent activation function, respectively.

It is known that the LSTM is employed to deal with the sequence-to-sequence data. However, apart from the time-series ground motions a_t, the input features also include the time-invariant random structural parameters. Herein, we first expand the time-invariant random structural parameters into a time-series sequence. At each time step t, the random structural parameters are the same:

$$
\mathbf{x}_S\left(t\right) = \left(\mathbf{x}_{S,0}, ..., \mathbf{x}_{S,t}, ..., \mathbf{x}_{S,T}\right) \tag{8}
$$

where $\mathbf{x}_{S,0} = \mathbf{x}_{S,t} = \mathbf{x}_{S,T}$. Then, the sequence of the random structural parameters can be concatenated with the time-series input feature, i.e., $(a_t, \mathbf{x}_{S,t})$. To distinguish, we denote the LSTM considering both the time-variant excitation and time-invariant random parameters as rLSTM, where the letter "r" represents the time-invariant random variables. The diagram is shown in Fig. 1 (b).

The concatenation of the random structural parameters sequence and the time-series ground motions leads to totally different scales in input features. Therefore, dataset normalization is required to ensure a stable and efficient training process. Consider a dataset $\mathcal{D} = \{a\left(t\right), \mathbf{x}_S\left(t\right), y\left(t\right)\}$, where $y\left(t\right)$ is the output time history responses of interest. The following normalization process is employed to scale input features and output responses:

$$
\begin{aligned}
&\tilde{a}\left(t\right) = a\left(t\right) / a_{\mathcal{D},\max} \\
&\tilde{y}\left(t\right) = y\left(t\right) / y_{\mathcal{D},\max} \\
&\tilde{\mathbf{x}}_S\left(t\right) = \left(\mathbf{x}_S\left(t\right) - \boldsymbol{\mu}_S\right) / \boldsymbol{\sigma}_S
\end{aligned}
\tag{9}
$$

where $a_{\mathcal{D},\max}$ and $y_{\mathcal{D},\max}$ are the maximum absolute ground motion and response in Dataset $\mathcal{D}$, respectively. $\boldsymbol{\mu}_S$ and $\boldsymbol{\sigma}_S$ are mean and standard deviation vector of random structural parameters $\mathbf{X}_\mathbf{S}$, respectively. Then, the dataset after preprocessing can be employed for training rLSTM. The rLSTM network is depicted in Fig. 2, where the notation

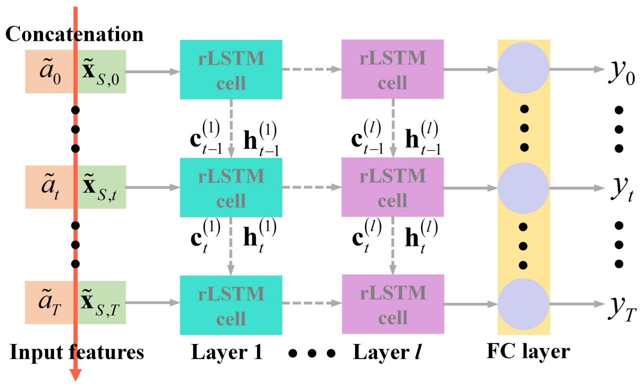

Figure 2: rLSTM network

"FC" refers to the fully connected neural network layers. It can be seen that the input feature is a concatenation of time-variant and time-invariant features and the network contains l rLSTM layers and the fully connected layer. The rLSTM network can circumvent the high-dimensional random variables for generating the seismic excitation (phase angles ϕ_ks) and employ the excitation as the pertinent input feature. Therefore, the rLSTM network can build metamodel for high-dimensional stochastic dynamic systems. Moreover, no matter which kind of approach is adopted for simulating the stochastic excitation (e.g., spectral representation method and random function-based spectral representation [54]), the proposed rLSTM can always be capable of constructing the metamodel since the ground motions serve as the pertinent input features.

3. Low-dimensional latent space identification for stochastic dynamic systems by rLSTM-AE

Different from the conventional surrogate models, e.g., Kriging model (Gaussian process regression), polynomial chaos expansion and etc., the proposed rLSTM network makes it available to build surrogates for high-dimensional stochastic dynamic systems. However, reliability analysis for the stochastic dynamic system by the metamodel is still a challenging issue. To conduct reliability analysis, a high-accuracy metamodel across the whole space is required to assess the failure probability. However, deep learning tools may require a substantial number of observations to achieve such a high accuracy across the whole domain. This challenge is also encountered by GPR model or PCE for low-dimensional reliability analysis especially when complex engineering problems are of concern. To tackle this issue, the active learning technique is widely used to convert the regression problem across the whole space into a classification problem focusing on the limit state surface. Unfortunately, this active learning-based reliability analysis is not available for high-dimensional reliability analysis due to the dimension limitation of the GPR model. Therefore, it is of importance to extract low-dimensional features for the high-dimensional stochastic dynamic systems. In this section, a low-dimensional latent space detection paradigm (rLSTM with autoencoder termed rLSTM-AE) and its application to the active leaning-based reliability analysis for high-dimensional stochastic dynamic systems is developed.

3.1. Active learning strategy for reliability analysis

Denote a performance function as:

$$W = G\left(\mathbf{X}\right) \tag{10}$$

where $\mathbf{X}$ is a vector of d number of random variables with a joint PDF $f_{\mathbf{X}}\left(\mathbf{x}\right)$. The failure probability can be calculated by:

$$P_f = \int_{\Omega_F} f_{\mathbf{X}}\left(\mathbf{x}\right) \mathrm{d}\mathbf{x} = \int_{\Omega} I\left(\mathbf{x}\right) f_{\mathbf{X}}\left(\mathbf{x}\right) \mathrm{d}\mathbf{x} \tag{11}$$

where $\Omega \subseteq \mathbb{R}^d$ and Ω_F is the failure domain defined by $\{\mathbf{x}|G\left(\mathbf{x}\right) < 0\}$. $I\left(\mathbf{x}\right)$ is an indicator function and $I\left(\mathbf{x}\right) = 1$ if $\mathbf{x} \in \Omega_F$, otherwise $I\left(\mathbf{x}\right) = 0$. MCS is a benchmark method for estimating Eq. (11):

$$P_f \approx \hat{P}_f = \sum_{i=1}^{N_{\mathrm{MC}}} \frac{I\left(\mathbf{x}^i\right)}{N_{\mathrm{MC}}} \tag{12}$$

where $\left\{\mathbf{x}^i, i = 1, 2, ..., N_{\mathrm{MC}}\right\}$ are N_{MC} samples drawn from the joint PDF $f_{\mathbf{X}}\left(\mathbf{x}\right)$. The coefficient of variation (CoV) can be given as:

$$\mathrm{CoV}\left(\hat{P}_f\right) = \sqrt{\frac{1 - \hat{P}_f}{N_{\mathrm{MC}} \times \hat{P}_f}} \tag{13}$$

However, numerous samples are required to achieve an accurate estimation and it is impossible for complex systems. To address this issue, surrogate models are widely adopted to replace the time-consuming performance function. However, it is still hard to build an accurate surrogate model across the entire space. Fortunately, the development of the active learning strategy enables the meatamodel to focus on the accuracy of the limit state surface.

An active learning reliability method combining Kriging model and Monte Carlo simulation termed AK-MCS has gained increasing popularity in recent years [2]. AK-MCS aims to accurately construct the limit state surface by Kriging model. The training dataset is adaptively enriched through a learning function by adding samples in the vicinity of the limit state surface. Hence, AK-MCS places emphases on the accuracy of the metamodel for the limit state surface but not the whole space. Regarding points far away from the limit state surface, the exact values of them are not required to be accurately predicted by metamodel as long as their signs are correctly identified. The active learning strategy leverages the elegant stochastic property of Gaussian process, that is, GPR not only provides the mean prediction at $\mathbf{x}$ but also quantifies the uncertainty associated with this prediction. The posterior distribution of the prediction at point $\mathbf{x}$, i.e., $\hat{G}(\mathbf{x})$, follows a normal distribution:

$$\hat{G}(\mathbf{x}) \sim \mathcal{N}\left(\mu_{\mathrm{g}}(\mathbf{x}), \sigma_{\mathrm{g}}^{2}(\mathbf{x})\right) \tag{14}$$

where $\mu_{\mathrm{g}}(\mathbf{x})$ and $\sigma_{\mathrm{g}}^{2}(\mathbf{x})$ are mean prediction and variance by GPR, respectively. The notation $\mathcal{N}$ denotes the normal distribution. This property has promoted the proposal of various learning functions. The learning function aims to select a best next point that can significantly improve the accuracy of the current metamodel. U learning function is widely used due to its simplicity:

$$U(\mathbf{x}) = \frac{|\mu_{\mathrm{g}}(\mathbf{x})|}{\sigma_{\mathrm{g}}(\mathbf{x})} \tag{15}$$

The value of U function reflects the probability of wrong classification in predicting the sign of $\mathbf{x}$, i.e., $\Phi(-U(\mathbf{x}))$. The notation Φ is the cumulative distribution function of the standard normal distribution. Therefore, a minimum value of U refers to the maximum risk of misclassification in predicting the sign of $\mathbf{x}$ so that the corresponding $\mathbf{x}$ should be selected and evaluated on the real performance function. Then, the training dataset for GPR can be enriched by adding this point with its true value. The procedure of the active learning-based MCS can be summarized as the follows:

Step 1: Genreate a MC candidate pool Ω with N_{MC} samples.

Step 2: Randomly select N_0 samples and evaluate them on the real performance function $G(\mathbf{X})$ as an initial training dataset $\{\mathbf{x}_{\mathrm{train}}, w_{\mathrm{train}}\}$, $w_{\mathrm{train}} = G(\mathbf{x}_{\mathrm{train}})$.

Step 3: Train the GPR with the current training dataset.

Step 4: Identify the best next point via the learning function and enrich the training dataset with $\{\mathbf{x}^*, w^*\}$:

$$\mathbf{x}^* = \underset{\mathbf{x}\in\Omega}{\arg\min}\, U(\mathbf{x}), w^* = G(\mathbf{x}^*) \tag{16}$$

Step 5: Stop the active learning process when the following condition is met, else go back to step 3:

$$\min(U(\mathbf{x})) \geq 2, \ \forall \mathbf{x} \in \Omega \tag{17}$$

This convergence condition represents that the maximum probability of misclassification on signs of all candidate samples is smaller than $\Phi(-2) = 2.3\%$, which can ensure the accuracy of the surrogate for the limit state surface.

Step 6: The updated GPR is utilized to predict values of samples in Ω and then the failure probability can be estimated by Eq. (12).

This active learning strategy significantly improves the accuracy and efficiency of GPR for reliability analysis. Commonly, GPR is not available for mapping sequence-to-sequence data. In this paper, the extreme value of time history responses of a stochastic dynamic system is of concern:

$$Y(t) = H(a(t), \mathbf{X}_S), Y_{\mathrm{ev}} = \max(\mathrm{abs}(Y(t))) \tag{18}$$

where $Y(t)$ represents the time history responses of interest, H denotes a high-dimensional stochastic system and Y_{ev} is the extreme response. Given a threshold b, the performance function gives:

$$W = b - Y_{\mathrm{ev}} = G(\mathbf{X}) \tag{19}$$

However, GPR is still not capable of constructing metamodel for high-dimensional systems even if the extreme responses are of interest, let alone the stochastic dynamic system investigated in this paper with more than 1000 random variables. Therefore, the active learning-based GPR is also not accessible to the reliability analysis of high-dimensional stochastic dynamic systems.

3.2. rLSTM with autoencoder for the low-dimensional latent space detection

To enable active learning-based GPR for high-dimensional problems, a fundamental idea is to use the dimension-reduction techniques. Moreover, the number of latent variables resulting from the dimension-reduction should be within several to dozens to ensure the availability and efficiency of GPR. Nevertheless, it is extremely hard for the stochastic

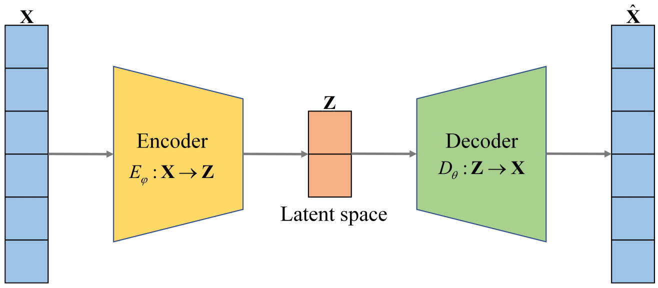

Figure 3: The diagram of autoencoder

dynamic system with more than 1000 features. To deal with thousands of input features, the neural networks-based features extraction technique can be a potential way. Autoencoder is a type of neural network for features extraction of unlabeled data and it is an unsupervised learning tool [41]. It includes an encoding function and a decoding function. The diagram of the autoencoder is depicted in Fig. 3, The encoding function aims to find efficient code or latent variables of unlabeled data, i.e., $E_{\boldsymbol{\varphi}} : \mathbf{X} \rightarrow \mathbf{Z}$ characterized by $\boldsymbol{\varphi}$. The decoding function is to recreate the input data via the latent variables, i.e., $D_{\boldsymbol{\theta}} : \mathbf{Z} \rightarrow \mathbf{X}$ characterized by $\boldsymbol{\theta}$. In theory, this kind of unsupervised learning-based neural network is available for low-dimensional latent variables detection of high-dimensional inputs. However, regarding the stochastic dynamic systems, we cannot use the input feature $\mathbf{X} = (\mathbf{X}_E, \mathbf{X}_S)$ directly for dimension-reduction due to the following three reasons:

Reason 1: random phases in vector $\mathbf{X}_E$ for generating the stochastic excitation are not pertinent features for a stochastic system and they have little effect on the response of interest.

Reason 2: random phases in vector $\mathbf{X}_E$ have equal contribution to the system since they all follow the same uniform distribution. Therefore, it is hard to detect several to dozens of latent variables to represent such a high-dimensional space with more than 1000 similar features.

Reason 3: even though the input features $\mathbf{X} = (\mathbf{X}_E, \mathbf{X}_S)$ could be represented by the low-dimensional latent variables $\mathbf{Z}$ directly, the time dependent property of the sequence-to-sequence data (time-dependent complex dynamics) is ignored when the detected latent variables is employed to construct a metamodel.

To tackle these issues, we propose a two-step low-dimensional latent variables detection strategy termed rLSTM-AE for the features extraction of a high-dimensional stochastic dynamic system. Commonly, the extreme value of the time-series response, i.e., $Y_{\mathrm{ev}} = \max\{\mathrm{abs}\,(Y\,(t))\}$, is of concern. The diagram of the proposed rLSTM-AE approach is depicted in Fig. 4.

As aforementioned, the proposed rLSTM network can deal with the stochastic excitation and random structural parameters simultaneously and well avoid the high-dimensional issue induced by the random phases $\mathbf{X}_E$. Therefore, the first step of the proposed rLSTM-AE is to find an approximate extreme value space by rLSTM, the dimension flow of this step is given by:

$$\mathbf{X} \in \mathbb{R}^{d_1+d_2} \xrightarrow{\mathrm{rLSTM}} Y_{\mathrm{ev}}^{\mathrm{rLSTM}} \in \mathbb{R}^1 \tag{20}$$

where $Y_{\mathrm{ev}}^{\mathrm{rLSTM}} = \max\left\{\mathrm{abs}\left(\hat{Y}\,(t)\right)\right\}$ and $\hat{Y}\,(t)$ is the time-series responses predicted by rLSTM. This step actually employs rLSTM to build a metamodel for the stochastic system and construct an approximate extreme value space, i.e., $Y_{\mathrm{ev}}^{\mathrm{rLSTM}}$. Note that the accuracy of this approximate extreme value space cannot be used for reliability analysis due to the limited observations for training rLSTM. We do not need a high-accuracy rLSTM here for reliability analysis since we just use this approximate one-dimensional space to find a low-dimensional latent space by autoencoder. Finally, active learning-based GPR will refine the estimated failure probability with the detected latent variables $\mathbf{Z}$. The loss function for training rLSTM can be defined by:

$$L\,(\boldsymbol{\lambda}) = \frac{1}{N}\sum_{i=1}^{N}\left\|y^i\,(t) - \hat{y}^i\,(\boldsymbol{\lambda}, t)\right\|_2^2 \tag{21}$$

where $\boldsymbol{\lambda}$ denotes trainable weights and biases of the rLSTM, which can be determined by $\hat{\boldsymbol{\lambda}} = \arg\min\limits_{\boldsymbol{\lambda}} L\,(\boldsymbol{\lambda})$. N is the

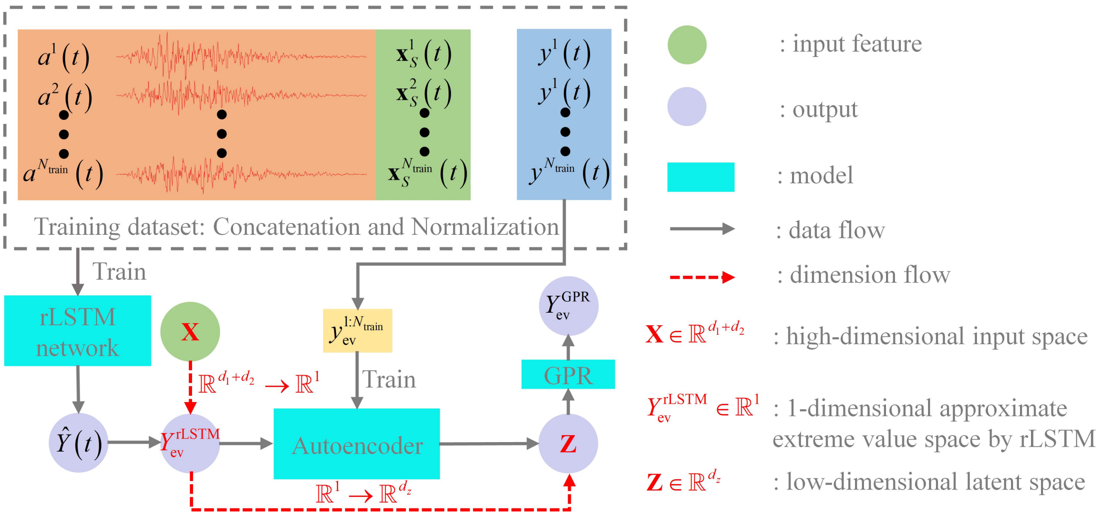

Figure 4: rLSTM-AE network

size of data and $\hat{y}(\lambda, t)$ is the estimated response. Note that the normalized data by Eq. (9) is utilized when training deep neural networks.

The second step for the proposed rLSTM-AE is to detect a low-dimensional latent space $\mathbf{Z}$ for decomposing the 1-dimensional extreme value space via autoencoder . Autoencoder in the rLSTM-AE network is different form its common use, the conventional autoencoder is an unsupervised learning method and the loss function can be defined as:

$$L(\boldsymbol{\varphi}, \boldsymbol{\theta}) = \frac{1}{N}\sum_{i=1}^{N} \left\| \mathbf{x}^i - D_{\boldsymbol{\theta}}\left(E_{\boldsymbol{\varphi}}\left(\mathbf{x}^i\right)\right) \right\|_2^2 \tag{22}$$

where $\{\boldsymbol{\varphi}, \boldsymbol{\theta}\}$ denotes the trainable weights and biases of the autoencoder, which can be determined by $\{\boldsymbol{\varphi}, \boldsymbol{\theta}\} = \arg\min_{\boldsymbol{\varphi}, \boldsymbol{\theta}} L(\boldsymbol{\varphi}, \boldsymbol{\theta})$. While for the autoencoder in the rLSTM-AE network, the loss function gives:

$$L(\boldsymbol{\varphi}, \boldsymbol{\theta}) = \frac{1}{N}\sum_{i=1}^{N} \left\| y_{\mathrm{ev}}^i - D_{\boldsymbol{\theta}}\left(E_{\boldsymbol{\varphi}}\left(y_{\mathrm{ev}}^i\right)\right) \right\|_2^2 \tag{23}$$

The encoding and decoding functions can be defined by $E_{\boldsymbol{\varphi}}: Y_{\mathrm{ev}} \to \mathbf{Z}$ and $D_{\boldsymbol{\theta}}: \mathbf{Z} \to Y_{\mathrm{ev}}$, respectively. Obviously, autoencoder here is adopted as a supervised learning tool. Note that when training autoencoder, real extreme responses is used since they can be provided by the training dataset. However, regarding the unobserved data, the real extreme responses are not available. Hence, the approximate extreme responses by rLSTM, i.e., $Y_{\mathrm{ev}}^{\mathrm{rLSTM}}$, are employed to detect the latent space $\mathbf{Z}$ for unobserved data. The dimension flow in this step can be expressed by:

$$Y_{\mathrm{ev}}^{\mathrm{rLSTM}} \in \mathbb{R}^1 \xrightarrow{\text{Autoencoder}} \mathbf{Z} \in \mathbb{R}^{d_z} \tag{24}$$

where d_z is the dimension of the latent variable $\mathbf{Z}$ and $d_z \geq 2$. The autoencoder here is to represent a 1-dimensional space by a d_z-dimensional latent space, which is a dimension-expansion step.

An important step is to determine an appropriate dimension of the potential latent space. Note that in this paper, the latent variable is employed to construct a GPR model so the dimension of $\mathbf{Z}$ is within the interval $[2, 20]$ to ensure the availability and efficiency of the active learning-based GPR. The basic idea of determining the dimension d_z is to ensure the accuracy of the reconstructed GPR model. Hence, in the proposed paradigm, the dimension of the latent variables d_z is adaptively determined by minimizing the following GPR reconstruction error:

$$L^{\mathrm{GPR}}(d_z) = \frac{1}{N}\sum_{i=1}^{N} \left\| y_{\mathrm{ev}}^i - \mathrm{GPR}\left(\mathbf{z}^i\right) \right\|_2^2, \mathbf{z} \in \mathbb{R}^{N \times d_z} \tag{25}$$

where $\mathbf{z}^i$ is the latent space corresponding to the observed data y_{ev}^i, i.e., $\mathbf{z}^i = E_{\boldsymbol{\varphi}}\left(y_{\text{ev}}^i\right)$. Then, the optimal dimension can be selected as:

$$d_z = \underset{2\leq d_z \leq 20}{\arg\min}\, L^{\text{GPR}}\left(d_z\right) \tag{26}$$

Therefore, Eq. (25) can help select a best latent space so that the GPR can reconstruct the extreme value space with the aid of the latent variable $\mathbf{Z}$.

There are three main steps for the proposed rLSTM-AE approach:

Step 1: The trained rLSTM can provide an approximate one-dimensional extreme value space for unobserved data:

$$Y_{\text{ev}}^{\text{rLSTM}} = \max\left(\text{abs}\left(\hat{Y}\left(t\right)\right)\right), \hat{Y}\left(t\right) = \text{rLSTM}\left(\left(a\left(t\right), \mathbf{X}_S\left(t\right)\right)\right) \tag{27}$$

Step 2: The one-dimensional approximate extreme value space can be decomposed by a trained autoencoder with the low-dimensional latent variables $\mathbf{Z}$:

$$\mathbf{Z} = E_{\boldsymbol{\varphi}}\left(Y_{\text{ev}}^{\text{rLSTM}}\right) \tag{28}$$

Step 3: The detected latent variables can be employed to construct a GPR metamodel, which can be used for the active learning-based reliability analysis.

$$Y_{\text{ev}}^{\text{GPR}} = \text{GPR}\left(\mathbf{Z}\right) \tag{29}$$

Actually, rLSTM-AE enables GPR to have the ability to predict extreme response as rLSTM and they have almost the same accuracy for predicting the extreme responses of a stochastic system, which will be validated in the following illustrative examples. Although this accuracy cannot satisfy the requirement of reliability analysis, GPR can be incorporated with the active learning strategy to improve the accuracy of failure probability estimation while rLSTM cannot. The proposed rLSTM-AE has the following three advantages corresponding to the aforementioned reasons 1$\sim$3 about why the autoenocder cannot be used directly:

Advantage 1: instead of the original high-dimensional input space $\mathbf{X}$, the pertinent feature, i.e., stochastic excitation $a\left(t\right)$, is concatenated with the sequential random structural parameters $\mathbf{X}_S\left(t\right)$ for the latent variables detection with the aid of the rLSTM.

Advantage 2: it is easy for the autoencoder to represent a one-dimensional space by several to dozens of latent variables.

Advantage 3: the time-dependent property in the sequence-to-sequence data (time-dependent complex dynamics) is taken into account by the rLSTM network during the dimension-reduction process.

Moreover, the proposed rLSTM-AE is not restricted by the way of generating stochastic excitation since the excitation is employed as the input feature directly. The observed dataset $\mathcal{D}$ generated by the Latin hypercube sampling is divided into two parts to obtain a best rLSTM-AE model. Training set with N_{train} samples aims to fit the parameters of the network and validation set with N_{valid} samples here is to select a best model during the learning process. Test set with N_{test} unobserved data generated by MCS is to assess the performance of the rLSTM-AE. Denote the dimension of input features as I_{dim}, the dimension of the output feature as O_{dim} and the size of hidden state as h_s. The detailed pseudo code for rLSTM-AE is indicated in Appendix A.

3.3. *rLSTM-AE for the active learning-based reliability analysis:* rLSTM-AE-ALGPR

Once the latent variables are identified by the proposed rLSTM-AE, they can be employed to construct a GPR metamodel and the active learning strategy is available for reliability analysis of high-dimensional stochastic dynamic systems. The core steps for the active learning approach expressed by Eq. (16) and (17) can be reformulated as:

$$\mathbf{z}^* = \min_{\mathbf{z}\in\Omega_{\mathbf{Z}}} U\left(\mathbf{z}\right) \tag{30}$$

and

$$\min\left(U\left(\mathbf{z}\right)\right) \geq 2,\ \forall \mathbf{z} \in \Omega_{\mathbf{Z}} \tag{31}$$

where $\Omega_{\mathbf{Z}} \subseteq \mathbb{R}^{d_z}$ is the latent candidate pool detected by rLSTM-AE from the original candidate pool $\Omega \subseteq \mathbb{R}^{d_1+d_2}$. Denote the GPR that combined with the rLSTM-AE and the active learning strategy as rLSTM-AE-ALGPR. The pesudo of rLSTM-AE-ALGPR is indicated in algorithm 1.

Algorithm 1 rLSTM-AE with the active learning-based GPR: rLSTM-AE-ALGPR

Input: Information of random variables, the response function H and performance function G.

Output: Failure probability $\hat{P}_f$.

1: Initiate a candidate pool $\Omega : \mathbf{x}_{\mathrm{CP}}$ with the sample size ΔN and the target CoV of $\hat{P}_f$, e.g., $\mathrm{CoV}_{\mathrm{tol}} = 5\%$.
2: Draw $N_{\mathrm{train}} + N_{\mathrm{valid}}$ samples from $f_{\mathbf{X}}(\mathbf{x})$ by Latin hypercube sampling, denoted as $\mathbf{x} = (\mathbf{x}_E, \mathbf{x}_S)$.
3: Generate the stochastic excitation $a(t)$ by $\mathbf{x}_E$ and Eq. (2).
4: Calculate the corresponding responses $y(t) = H(a(t), \mathbf{x}_S)$ and $y_{\mathrm{ev}} = \max(\mathrm{abs}(y(t)))$.
5: Generate the observed dataset $\{a(t), \mathbf{x}_S, y(t)\}$ and train rLSTM-AE via the algorithm 2.
6: Randomly select N_{GPR} samples form the observed dataset as the initial training set of GPR, i.e., $\left\{\mathbf{x}^{1:N_{\mathrm{GPR}}}, G\left(\mathbf{x}^{1:N_{\mathrm{GPR}}}\right)\right\}$.
7: Transform the initial training set into latent space by the trained rLSTM-AE: $\{\boldsymbol{\mathcal{Z}}, \mathcal{W}\} \leftarrow \left\{\mathbf{z}^{1:N_{\mathrm{GPR}}}, G\left(\mathbf{x}^{1:N_{\mathrm{GPR}}}\right)\right\} \leftarrow \left\{\mathbf{x}^{1:N_{\mathrm{GPR}}}, G\left(\mathbf{x}^{1:N_{\mathrm{GPR}}}\right)\right\}$.
8: **while** $\mathrm{CoV}\left(\hat{P}_f\right) > \mathrm{CoV}_{\mathrm{tol}}$ **do**
9: Transform the candidate pool into the latent space:$\Omega_{\mathbf{Z}} : \mathbf{z}_{\mathrm{CP}} \leftarrow \Omega : \mathbf{x}_{\mathrm{CP}}$.
10: **while** $\min(U(\mathbf{z}_{\mathrm{CP}})) < 2$ **do**
11: Build GPR via training set $\{\boldsymbol{\mathcal{Z}}, \mathcal{W}\}$ and evaluate $\mathbf{z}_{\mathrm{CP}}$ on GPR.
12: Calculate $U(\mathbf{z}_{\mathrm{CP}}) = \mu_G(\mathbf{z}_{\mathrm{CP}}) / \sigma_G(\mathbf{z}_{\mathrm{CP}})$.
13: Enrich $\{\boldsymbol{\mathcal{Z}}, \mathcal{W}\}$ by U learning function with the point corresponding to $\mathbf{z}^* = \min(U(\mathbf{z}_{\mathrm{CP}}))$, where the corresponding output is calculated in the original space, i.e., $G(\mathbf{x}^*)$.
14: **end while**
15: Calculate $\hat{P}_f$ and $\mathrm{CoV}\left(\hat{P}_f\right)$ by Eqs. (12) and (13), respectively.
16: Enrich the candidate pool Ω by adding ΔN samples.
17: **end while**
18: Output the failure probability $\hat{P}_f$.

The contribution of the proposed paradigm are listed as the follows:

1: The proposed rLSTM network utilizes the stochastic excitation as the pertinent input feature, which can circumvent the high-dimensional random phases for generating the excitation. Therefore, no matter which approach is employed for generating stochastic process, the rLSTM can be always available.

2: The rLSTM considers both the time-variant stochastic excitation and the time-invariant random structural parameters simultaneously, which makes it available to construct metamodel for the high-dimensional stochastic dynamic systems directly.

3: To address the insufficient accuracy of the rLSTM network (due to limited observations) for dynamic reliability analysis, the autoencoder is utilized to decompose the approximate one-dimensional extreme response with the aid of rLSTM, which brings insights for latent variables extraction from the perspective of output space decomposition.

4: The rLSTM-AE network for low-dimensional latent space detection considers the complex time-dependent dynamics of stochastic systems by the rLSTM while conventional dimension-reduction techniques ignore this issue.

5: The proposed method makes the active learning-based reliability analysis method available for the high-dimensional dynamic reliability analysis.

4. Illustrative Examples

A single-degree-of-freedom system (SDOF) and a 3D reinforced concrete frame structure subjected to the stochastic excitation are investigated in this section. The structures of the rLSTM and autoencoder are constructed by PyTorch. The structure of rLSTM-AE network is specified as follows. The number of LSTM layers for rLSTM network is specified as $l = 2$, one fully connected neural network layer is used and the size of hidden state is set as $h_s = 50$. The encoding function $E_{\boldsymbol{\varphi}}$ is a fully connected neural network that consists of three layers. Each layer contains $4d_z$, $2d_z$ and d_z nodes, respectively. The corresponding decoding function $D_{\boldsymbol{\theta}}$ is also a three-layer fully connected neural network and each layer contains $2d_z$, $4d_z$ and 1 nodes, respectively. The activation function is adopted as ReLU. In this paper, 1000 observed data generated by Latin hypercube sampling are employed, among which $N_{\mathrm{train}} = 800$ for training and $N_{\mathrm{valid}} = 200$ for validation. 10000 unobserved data generated by MCS is employed for testing the rLSTM-AE model. The ”fitrgp” function in MATLAB is used for constructing a GPR model, where the linear basis is adopted, the kernel function is set as “ardsquaredexponential” and the constant sigma is adopted as 0.001.

Regarding the reliability analysis problem of the high-dimensional stochastic systems investigated in this paper, MCS is adopted as the reference method. To the best of the authors' knowledge, there is no existing surrogate model that can be employed for this high-dimensional stochastic system directly due to the curse of dimensionality. The conventional metamodels such as polynomial chaos expansion, support vector regression and Gaussian process regression are all unavailable. The moment-based methods can be employed for comparisons since the extreme responses are of interest. Herein, the popular maximum entropy method (MEM) and a mixture distribution approach by combining inverse Gaussian and lognormal distribution termed MIGLD [33] are employed for the failure probability estimation of the stochastic dynamic system. The failure probabilities by the proposed metamodel (rLSTM) for the high-dimensional stochastic system, the Gaussian process regression with the detected latent variables by rLSTM-AE termed rLSTM-AE-GPR and the active learning-based GPR with the identified latent variables called rLSTM-AE-ALGPR are provided.

4.1. Example 1

A single-degree-of-freedom system modeled by the Bouc-Wen hypothesis shown in Fig. 5 is investigated [35]. The restoring force F of this system can be expressed by:

$$F(u, r) = k\left[qu + (1 - q)r\right] \tag{32}$$

where k is the stiffness and r is the hysteretic displacement following the Bouc-Wen hypothesis:

$$\dot{r} = A\dot{u} - B\left|\dot{u}\right|\left|r\right|^{e-1}r - C\dot{u}|r|^{e} \tag{33}$$

where the parameters are set to: $q = 0.2$, $A = 1$, $B = C = 5 \times 10^5$ and $e = 3$. Three random variables of the SDOF, i.e., the lumped mass m, the stiffness k and the viscous damping c are of concern. The mass m follows a normal distribution with mean 41000 kg and a CoV of 0.1. The stiffness k follows a lognormal distribution with mean 1.5×10^6 N/m and a CoV of 0.2. The damping c is a lognormal distribution with mean $4.35 \times 10^4\ \mathrm{N \cdot s/m}$ and a CoV of 0.2. The detail of spectrum representation method for generating the stochastic ground motions is provided in

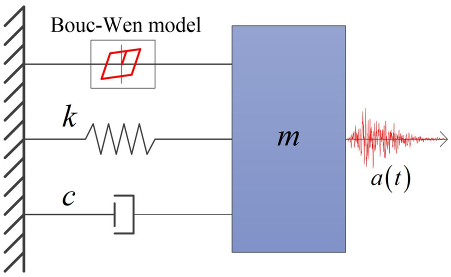

Figure 5: A single-degree-of-freedom system modeled by Bouc-Wen hypothesis

section 2.1. Therefore, this system has three random structural parameters and 1001 random phases for generating the stochastic excitation so it is a high-dimensional problem with 1004 input random variables. The mean and standard deviation of the fully non-stationary stochastic excitation simulated by 1000 Latin hypercube samples are shown in Fig. 6 (a) and (b), respectively. The simulated ones are in good accordance with the target ones, which indicates that the 1000 samples generated by Latin hypercube sampling can well simulate the stochastic excitation. The time history displacement of the SDOF is of interest.

These 1000 observations are used to train the rLSTM-AE network. The training loss and validation loss by LSTM-GM and rLSTM are shown in Fig. 7, where the notation “LSTM-GM” represents that only the stochastic ground motions serve as the input features for training. It can be observed that there is an obvious gap between the loss by

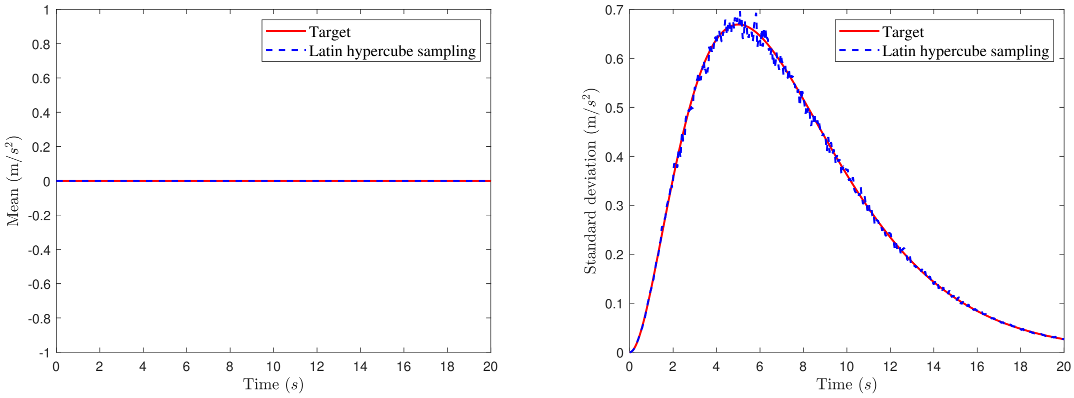

(a) Mean (b) Standard deviation

Figure 6: Mean and standard deviation of the fully non-stationary stochastic ground motions

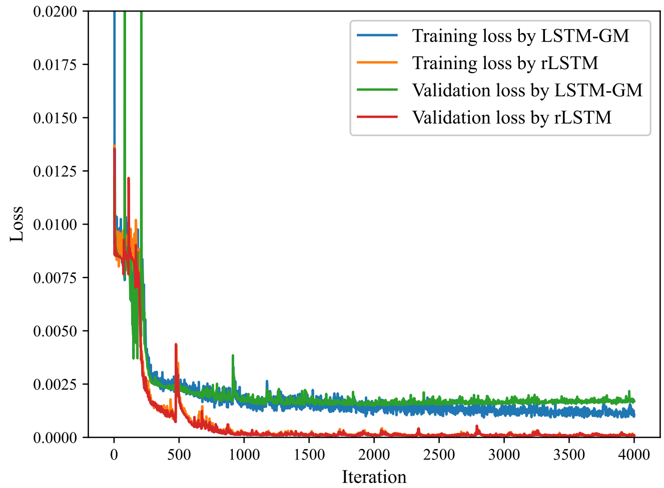

Figure 7: Training and validation loss in example 1

LSTM-GM and loss by rLSTM since LSTM-GM ignores the time-invariant random structural parameters, which indicates that the uncertainties of structural parameters also play an important role in the stochastic system. Hence, the proposed rLSTM provides a direct way for metamodeling of the high-dimensional stochastic systems considering both time-variant and time-invariant random variables. Four representative time history responses predicted by the rLSTM and LSTM-GM are depicted in Fig. 8. The red dashed line by rLSTM accords well with the ground truth, i.e., the black line. The blue line by LSTM-GM shows quite different time history responses compared with the true ones, which manifests that the importance of the time-invariant random structural parameters again.

The extreme responses are of interest, Fig. 9 (a) depicts predictions of training and validation datasets and (b) shows predictions of 10000 test samples. The green and black dashed lines show the relative errors of 10% and 20% compared with the ground truth, respectively. The determination coefficient R^2 by the rLSTM network is also provided in the figure. It can be seen that the trained rLSTM network can fit the 1000 observed data and 10000 unobserved test data well. The relative errors of predictions on the test set are mainly within the 10% bound and the R^2 is close to 1, i.e., 0.9745. The results indicate that the proposed rLSTM network can construct a fairly good metamodel for the stochastic

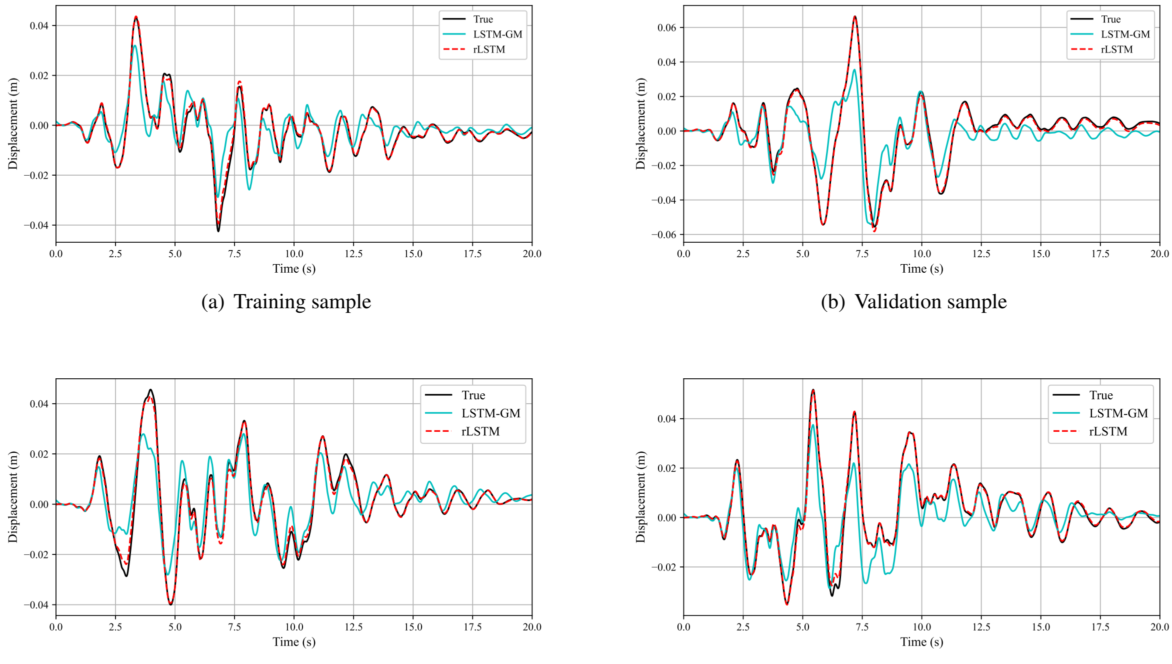

(a) Training sample

(b) Validation sample

(c) Test sample 1

(d) Test sample 2

Figure 8: Representative samples predicted by rLSTM in example 1

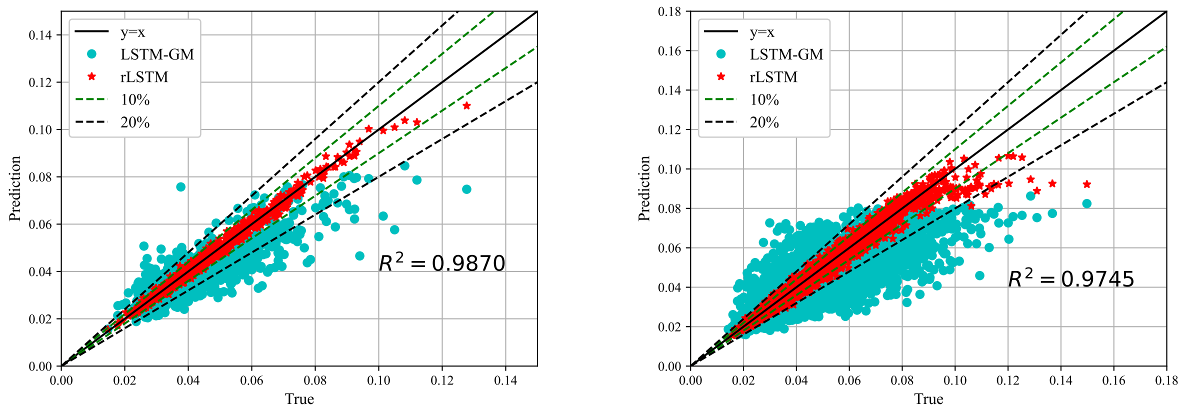

(a) Training and validation (1000 samples)

(b) Test (10000 samples)

Figure 9: Predictions on extreme responses in example 1

system with 1004 input random variables. Herein, the K-fold cross validation method is also employed to validate the generalization ability of the proposed rLSTM, where 5 folds are adopted. The determination coefficients are 0.9710, 0.9753, 0.9769, 0.9410 and 0.9687, respectively, which are all close to 1. The average determination coefficient is 0.9666, which indicates the generalization ability of the proposed rLSTM. Furthermore, the probability density function (PDF) of the extreme responses and the curve of the probability of exceedance (POE) in logarithmic scale by the proposed rLSTM (obtained from predictions on 10^5 unobserved samples) are shown in Fig. 10 (a) and (b), respectively,

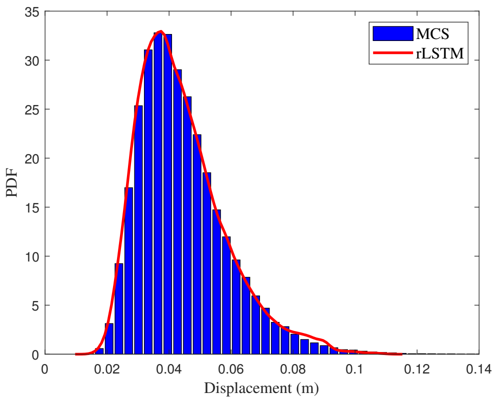

(a) PDF (b) POE

Figure 10: PDF and POE of the extreme responses predicted by rLSTM in example 1

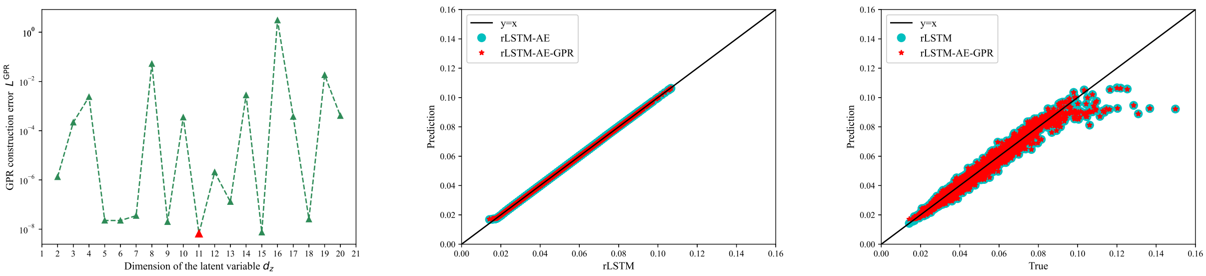

(a) GPR reconstruction error (b) Compared with the rLSTM (c) Compared with the ground truth

Figure 11: Performance of rLSTM-AE and rLSTM-AE-GPR

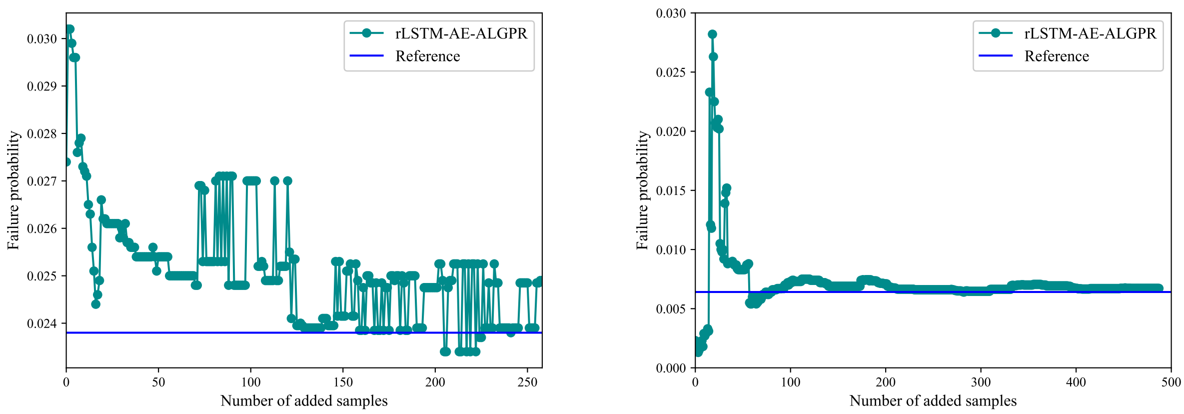

(a) Case 1 (b) Case 2

Figure 12: Failure probability estimation in example 1

Table 1: Results obtained by different methods in example 1

	Method	N_{call}	P_f	$\text{CoV}(P_f)$	R.E.
Case 1	MCS	1×10^5	2.38×10^{-2}	2.03%	–
	MEM	1000	2.94×10^{-2}	–	23.53%
	MIGLD	1000	2.70×10^{-2}	–	13.58%
	rLSTM	1000	2.58×10^{-2}	4.35%	8.40%
	rLSTM-AE-GPR	1000	2.58×10^{-2}	4.35%	8.40%
	rLSTM-AE-ALGPR	1258	2.49×10^{-2}	4.42%	4.62%
Case 2	MCS	1×10^5	6.41×10^{-3}	3.94%	–
	MEM	1000	9.23×10^{-3}	–	43.96%
	MIGLD	1000	7.13×10^{-3}	–	11.25%
	rLSTM	1000	2.88×10^{-3}	5.88%	55.07%
	rLSTM-AE-GPR	1000	2.88×10^{-3}	5.88%	55.07%
	rLSTM-AE-ALGPR	1487	6.72×10^{-3}	4.96%	4.78%

where the reference results are by 10^5 MCS. It can be seen that the rLSTM can capture the main body of the distribution while the accuracy of the tail is insufficient since the accuracy of the metamodeling for the high-dimensional stochastic dynamic system across the whole domain is hard to be achieved with the limited observations. Therefore, we need to detect a low-dimensional latent space to construct an active learning-based GPR for failure probabilities estimation with the aid of the rLSTM.

The extreme responses of the 1000 observed data are also employed to train the autoencoder, where $N_{\text{train}} = 800$, $N_{\text{valid}} = 200$ and the size of the training set for GPR is $N_{\text{GPR}} = 100$ as indicted in algorithm 2. To determine the best dimension of the latent space, as indicated in algorithm 2, we first specify the dimension from 2 to 20 and then the structure of the autoencoder can be determined accordingly.The autoencoder is trained based on the observed data. Then, the best autoencoder model and the so-called GPR reconstruction error corresponding to the d_z are saved. Finally, after training the autoencoder with d_z from 2 to 20, the minimum GPR reconstruction error can be found and the best dimension of the latent space is determined accordingly. The error of the GPR construction with respect to the dimension d_z is plotted in Fig. 11 (a). The red point denotes the minimum error so the best dimension of the latent space is $d_z = 11$ in this example. Fig. 11 reflects the accuracy of the autoencoder or GPR for the approximate extreme value space (extreme responses obtained by rLSTM) reconstruction. The accuracy is validated on 10000 test samples. The horizontal axis represents the extreme responses estimated by rLSTM and the vertical axis denotes predictions by the trained autoencoder or GPR with the low-dimensional latent variables obtained from the trained autoencoder. It can be found the trained autoencoder (rLSTM-AE) can accurately reconstruct the extreme space approximated by rLSTM, which means that the detected latent variables well capture the features of the extreme space by rLSTM. It is mainly because the autoencoder can easily detect d_z features for a one-dimensional space. Therefore, the GPR with the detected latent variables by rLSTM-AE termed rLSTM-AE-GPR can also accurately reconstruct the approximate extreme space. This step enables the GPR to predict the extreme responses and achieve the same accuracy as the rLSTM network. This conclusion can also be seen from Fig. 11 (c). The extreme responses predicted by rLSTM and rLSTM-AE-GPR are compared with the ground truth. The accuracy of the GPR is almost the same as the rLSTM regarding the extreme responses estimation. Although the accuracy is insufficient for reliability analysis, rLSTM-AE-GPR can leverage the active learning strategy to improve the failure probability estimation while the rLSTM cannot.

Two cases corresponding to the thresholds of 80 mm and 95 mm are of concern. The size of the initial training set for GPR is set to $N_{\text{GPR}} = 100$. The active learning processes are shown in Fig. 12 (a) and (b), respectively. It can be found that the estimated failure probability converges to the reference along with the enrichment of the training set. The results by different methods are listed in Table 1, where N_{call} represents the number of calls to the stochastic system and the notation "R.E." denotes the relative error of the estimated failure probability. Regarding the case 1, the failure probabilities by MEM and MIGLD are not as accurate as the proposed rLSTM-based methods. rLSTM and the rLSTM-AE-GPR achieve the same accuracy since the GPR constructed by the detected latent variables has the same ability to predict the extreme response as rLSTM, which is consistent with the results shown in Fig. 11 (c). However, as stated before, the accuracy of the rLSTM network is insufficient for reliability analysis due to the limited observations for constructing a metamodel across the whole domain. The relative errors by rLSTM and rLSTM-AE-GPR are both 8.40% in case 1. By leveraging the active learning strategy, rLSTM-AE-ALGPR produces a more accurate failure probability, i.e., the relative error is 4.62%. Note that 1000 observed samples are employed for training rLSTM-AE network and 258 training samples are identified by the U learning function so the total number of calls is 1258 for rLSTM-AE-ALGPR. When considering a small failure probability in case 2, i.e., 6.41×10^{-3} by 10^5 MCS, the MEM, MIGLD, rLSTM, rLSTM-AE-GPR cannot produce satisfactory results. The relative errors by rLSTM and rLSTM-AE-GPR are both as large as 55.07%. With the aid of the active learning approach, rLSTM-AE-ALGPR can obtain a fairly good accuracy, the relative error of the failure probability is reduced to 4.78% from 55.07% by adaptively adding 487 samples. Furthermore, a small failure probability corresponding to a threshold of 125 mm is of concern in this example. To obtain a reliable estimation, 10^6 MCS is employed and the reference failure probability is 3.77×10^{-4}. Actually, it is known that MCS is not a good way for the active learning-based small failure probability estimation since a substantial number of samples are required to ensure a reliable estimation [17, 55]. Active learning training with a large candidate pool is computationally expensive. This issue becomes more serious in the context of the stochastic dynamics since generating the stochastic excitation is also time-consuming. Some advanced sampling techniques such as the importance sampling and subset sampling are combined with the active learning for reliability analysis of low-dimensional static systems [17, 55]. However, the combination of the more advanced sampling approaches with the proposed high-dimensional active learning strategy should be further investigated for small failure probability estimation. In this example, 10^6 MCS is adopted as the candidate pool and combined with the proposed active learning strategy. The whole candidate pool is divided into 5 groups based on the peak ground motions and 1000 samples are randomly selected from the 5 groups as the training set. The failure probability by rLSTM and rLSTM-AL-GPR are 9.01×10^{-5} and 8.93×10^{-4}, respectively, which significantly deviate from the reference result. With the aid of the proposed high-dimensional active learning strategy, the accuracy of the failure probability estimation is remarkably improved by the proposed method, the failure probability by rLSTM-AE-ALGPR is 2.96×10^{-4}. In this paper, the proposed active learning strategy with the crude MCS is studied so it is suggested to employ the proposed method for a relatively large failure probability estimation.

4.2. Example 2

To validate the proposed method for the practical engineering problems, a 3D reinforced concrete frame structure subjected to the fully non-stationary stochastic seismic excitation is investigated [56]. The structural configuration and reinforcement information are shown in Fig. 13. The finite element model is constructed by OpenSees and the constitutive laws Concrete01 and Steel01 are adopted. 7 random structural variables are involved and listed in Table 2. Therefore, the total number of the input random variables is 1008 in this example. The time history displacement at point A in the Fig. 13 is of interest.

Table 2: Random variables in example 2

Variable	Description	Distribution	Mean	CoV
f_c	Concrete compressive strength	Lognormal	26.8 MPa	0.20
ε_c	Concrete strain at maximum strength	Lognormal	0.0015	0.05
f_u	Concrete crushing strength	Lognormal	10 MPa	0.20
ε_u	Concrete strain at crushing strength	Lognormal	0.0033	0.05
f_y	Yield strength of rebar	Lognormal	400 MPa	0.20
E_0	Initial elastic modulus of rebar	Lognormal	206 GPa	0.20
b	Strain-hardening ratio of rebar	Lognormal	0.01	0.05

Similarly, 1000 observed data are employed to train rLSTM-AE network. The training and validation losses by rLSTM and LSTM-GM are shown in Fig. 14. There is always a gap between LSTM-GM and rLSTM throughout the training process, which states that the uncertainties of structural parameters are critical to the response of interest. Hence, rLSTM considers both time-variant and time-invariant input features is necessary for the metamodel construction of

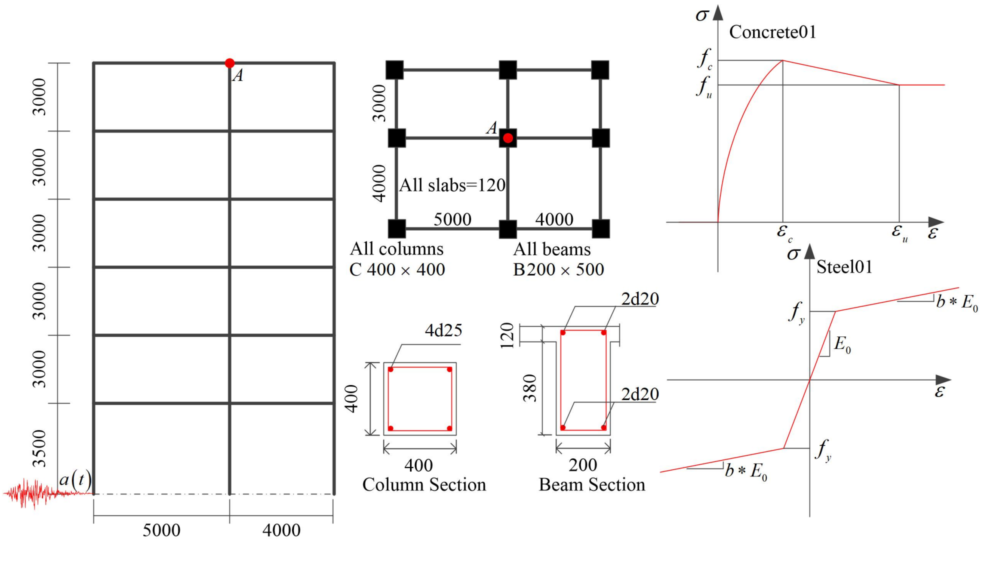

Figure 13: The 3D reinforced concrete frame structure

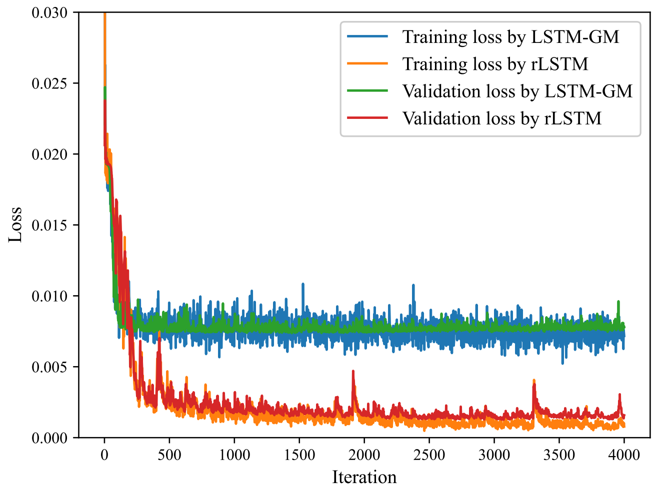

Figure 14: Training and validation loss in example 2

stochastic dynamic systems. Four representative samples are presented in Fig. 15, which proves again that the rLSTM has a better performance than LSTM-GM. Fig. 16 (a) shows the accuracy of the extreme responses predicted by rLSTM and LSTM-GM on training and validation datasets. Fig. 16 (b) showcases the accuracy of the extreme responses predicted on 10000 test samples. It can be observed that the relative errors of the predicted samples by rLSTM are predominately below 20% while the accuracy of the blue samples predicted by LSTM-GM is unsatisfactory. The determination coefficient calculated by rLSTM on 10000 test samples is close to 1, which states that the rLSTM can achieve a pretty good accuracy. The K-fold cross validation is utilized to further validate the generalization ability of the proposed rLSTM and the determination coefficients are 0.9414, 0.9369, 0.9445, 0.8831 and 0.9141, respectively. The mean R^2 is 0.9240, which is close to 1. Hence, the generalization ability of the rLSTM is validated again. Moreover, the PDF and POE in logarithmic scale by 10^5 MCS are depicted in Fig. 17, which manifests that the rLSTM can well capture the main body of the extreme responses distribution. The rLSTM loses some accuracy in the tail of the

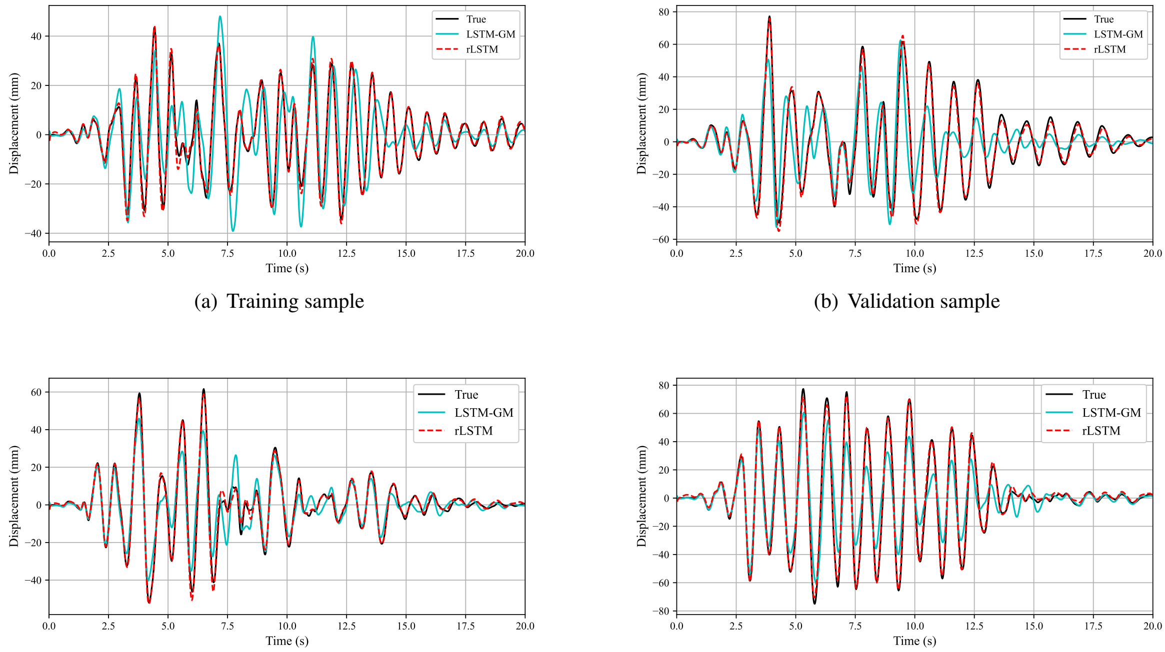

(a) Training sample (b) Validation sample

(c) Test sample 1 (d) Test sample 2

Figure 15: Representative samples predicted by rLSTM in example 2

distribution since it is hard to build a metamodel for the stochastic dynamic system across the whole domain with the limited observations.

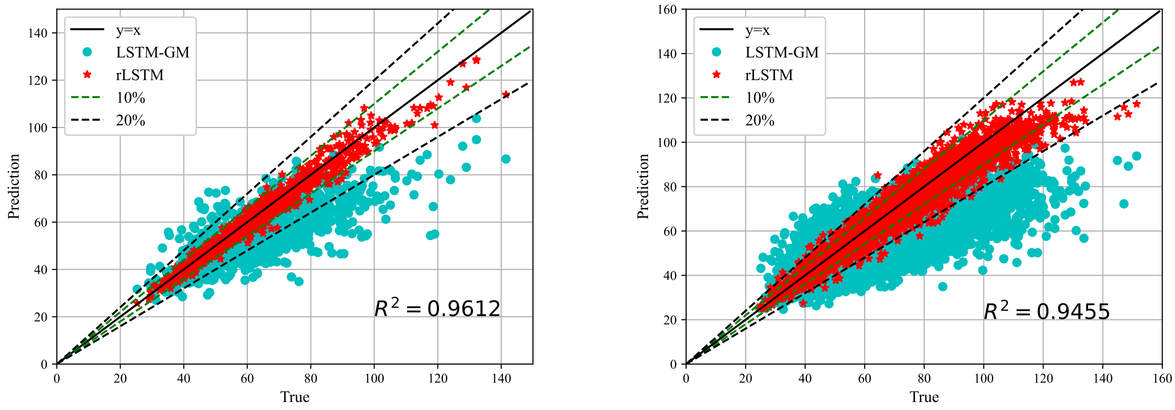

(a) Training and validation (1000 samples) (b) Test (10000 samples)

Figure 16: Predictions on extreme responses in example 2

Regarding the reliability analysis of this 1008-dimensional stochastic dynamic system, the low-dimensional latent variables are required to be identified since the accuracy of the rLSTM is still insufficient for the failure probability estimation with the current limited observations. Then, the active learning-based GPR metamodel can be constructed to

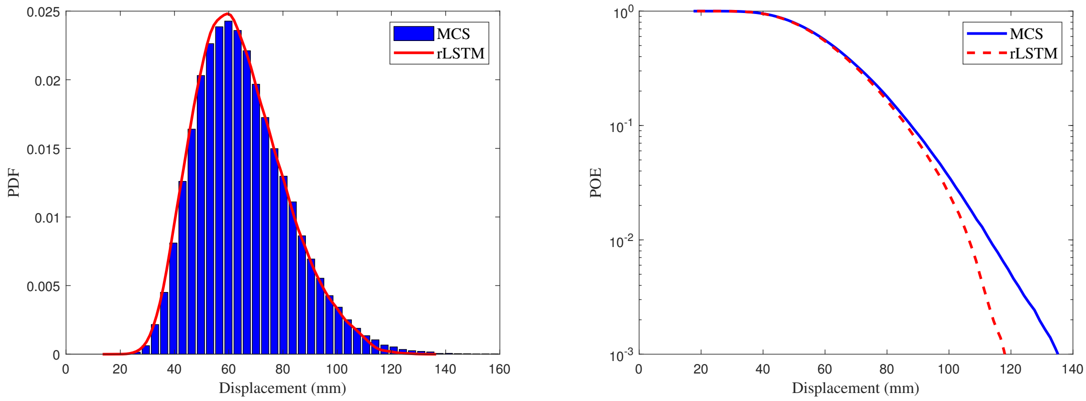

(a) PDF (b) POE

Figure 17: PDF and POE of the extreme responses predicted by rLSTM in example 2

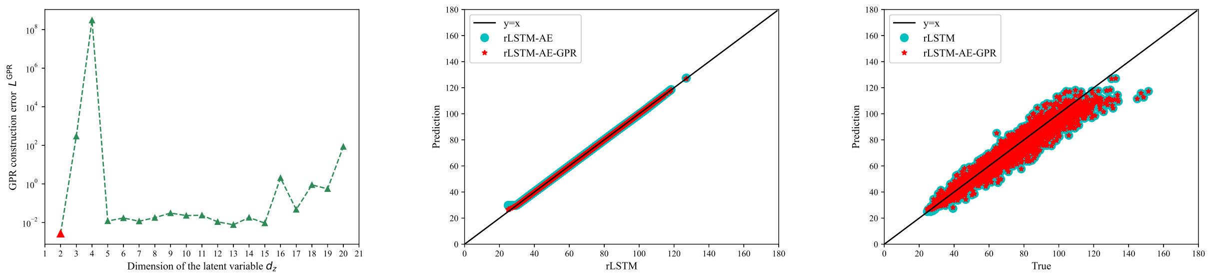

(a) GPR reconstruction error (b) Compared with the rLSTM (c) Compared with the ground truth

Figure 18: Performance of rLSTM-AE and rLSTM-AE-GPR

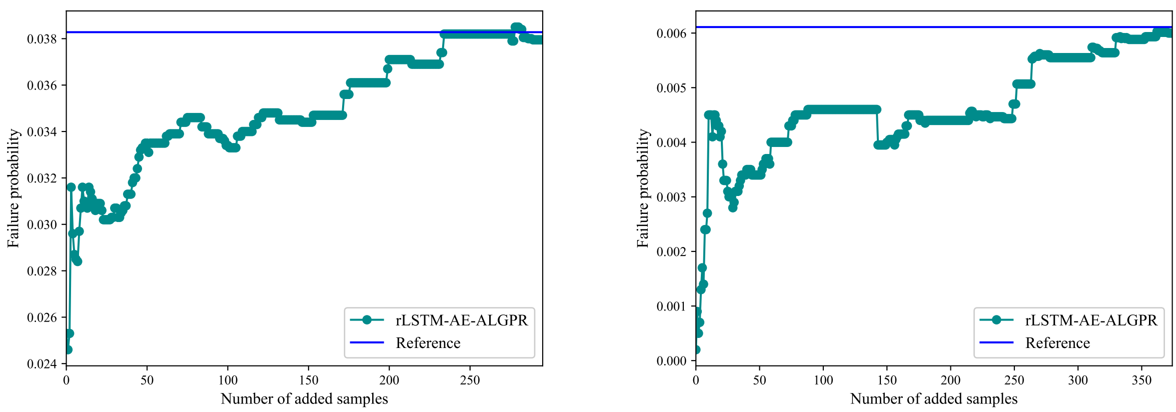

(a) Case 1 (b) Case 2

Figure 19: Failure probability estimation in example 2

Table 3: Results obtained by different methods in example 2

	Method	N_{call}	P_f	$\text{CoV}(P_f)$	R.E.
Case 1	MCS	1×10^5	3.83×10^{-2}	1.59%	–
	MEM	1000	3.43×10^{-2}	–	10.28%
	MIGLD	1000	3.52×10^{-2}	–	8.01%
	rLSTM	1000	2.56×10^{-2}	4.36%	33.12%
	rLSTM-AE-GPR	1000	2.56×10^{-2}	4.36%	33.12%
	rLSTM-AE-ALGPR	1295	3.80×10^{-2}	3.56%	0.86%
Case 2	MCS	1×10^5	6.11×10^{-3}	4.03%	–
	MEM	1000	6.49×10^{-3}	–	6.13%
	MIGLD	1000	6.35×10^{-3}	–	3.85%
	rLSTM	1000	9.40×10^{-4}	10.31%	84.62%
	rLSTM-AE-GPR	1000	9.30×10^{-4}	10.36%	84.78%
	rLSTM-AE-ALGPR	1374	6.00×10^{-3}	4.86%	1.80%

improve the reliability analysis process. Fig. 18 (a) depicts the GPR construction error with respect to the dimension of the latent variables d_z. It can be found that $d_z = 2$ is the best dimension for constructing a GPR metamodel in this example. Fig. 18 (b) presents the performance of the trained autoenoder and rLSTM-AE-GPR on reconstructing the extreme responses by rLSTM. Both of them achieve high-accuracy, which manifests that the GPR with the latent variables detected by rLSTM-AE can perfectly reconstruct the extreme value space predicted by the rLSTM. Fig. 18 (c) showcases that the rLSTM-AE-GPR is equivalent to the rLSTM regarding the extreme responses estimation. Then, rLSTM-AE-GPR can combine the active learning strategy for the failure probability estimation. In this example, two cases corresponding to the thresholds of 100 mm and 119 mm are of concern. Fig. 19 shows the active learning process for failure probabilities estimation. With the aid of the active learning, the accuracy of the estimated failure probability increases with the enrichment of training set and the final failure probability converges to the benchmark by MCS.

Moreover, the failure probabilities by different methods are listed in Table 3. For case 1, the relative errors by MEM and MIGLD are larger than 5%. rLSTM and rLSTM-AE-GPR do not produce satisfactory results and the relative errors of the failure probability are as large as 33.12%, which results from the insufficient accuracy of the rLSTM for reliability analysis under limited observations. rLSTM-AE-ALGPR produces an accurate failure probability by adaptively adding 295 samples and the relative error is as small as 0.86%. Regarding case 2, the reference failure probability i.e., 6.11×10^{-3} is produced by 10^5 MCS. MIGLD obtains more accurate result than MEM by consuming the same number of function calls. Again, the accuracy of the rLSTM and rLSTM-AE-GPR is not sufficient for reliability analysis and the relative errors are both over 80%. By leveraging the active learning, the training set for GPR construction is enriched by 374 samples and the accuracy of the estimated failure probability is significantly improved. The relative error is reduced to 1.8% from 84.62% compared with the rLSTM.

5. Concluding Remarks

In this paper, a rLSTM network considering both time-variant and time-invariant input features for metamodeling of the high-dimensional stochastic dynamic systems is developed. The stochastic excitation is employed as the pertinent input but not the random phases for simulating the excitation. The proposed rLSTM is capable of capturing the main body of the extreme response distribution of a high-dimensional stochastic dynamic system by consuming the limited observations. Regarding the reliability analysis, it is usually hard to build a high-accuracy metamodel across the whole domain under the limited training samples. To surmount the insufficient accuracy of reliability analysis induced by the limited observations, the rLSTM is combined with the autoencoder to detect a low-dimensional latent space of the approximate extreme value space. The best latent space for reconstructing the approximate extreme value space is selected by minimizing the error between the GPR predictions and the ground truth. Finally, the active learning-based GPR is combined with the latent variables to improve the accuracy of failure probabilities estimation. The results of a 1004-dimensional SDOF system and a 1008-dimensional reinforced concrete frame structure subjected to the stochastic excitation validate that the proposed method is capable of building metamodel and accurately approximating the failure probability for the high-dimensional stochastic dynamic systems. The proposed rLSTM provides a way of metamodeling for a stochastic dynamic system with more than 1000 input features. The rLSTM-AE brings insights for the low-dimensional features extraction from the perspective of the approximate output space, which makes the active learning-based reliability analysis available for the high-dimensional stochastic dynamic systems. It is recommended to employ the proposed rLSTM-AE-ALGPR with the crude MCS for a relatively large failure probability estimation. Future study will focus on combining the more advanced sampling techniques with the proposed high-dimensional active learning strategy for the small failure probabilities estimation.

CRediT authorship contribution statement

Yu Zhang: Conceptualization, Methodology, Investigation, Writing - original draft. **You Dong:** Conceptualization, Investigation, Writing – review & editing. **Michael Beer:** Conceptualization, Investigation, Writing – review & editing

Declaration of competing interest

The authors declare that they have no known competing financial interests or personal relationships that could have appeared to influence the work reported in this paper.

Acknowledgments

This study has been supported by the National Natural Science Foundation of China (Grant No. 52078448), and the Research Grants Council of the Hong Kong Special Administrative Region, China (No. PolyU 15221521 and PolyU 15225722).

Appendix A. The pseudo code of rLSTM-AE for latent variables detection

References

[1] G. Blatman, B. Sudret, An adaptive algorithm to build up sparse polynomial chaos expansions for stochastic finite element analysis, Probabilistic Engineering Mechanics 25 (2010) 183–197.
[2] B. Echard, N. Gayton, M. Lemaire, AK-MCS: an active learning reliability method combining Kriging and Monte Carlo simulation, Structural Safety 33 (2011) 145–154.
[3] S. Chandra, V. Matsagar, S. Marburg, Stochastic dynamic analysis of composite plates in thermal environments using nonlinear autoregressive model with exogenous input in polynomial chaos expansion surrogate, Computer Methods in Applied Mechanics and Engineering 416 (2023) 116303.
[4] D. Xiu, G. E. Karniadakis, The Wiener–Askey polynomial chaos for stochastic differential equations, SIAM journal on scientific computing 24 (2002) 619–644.
[5] R. G. Ghanem, P. D. Spanos, Stochastic finite elements: a spectral approach, Courier Corporation, 2003.
[6] C. Soize, R. Ghanem, Physical systems with random uncertainties: chaos representations with arbitrary probability measure, SIAM Journal on Scientific Computing 26 (2004) 395–410.
[7] L. Cao, J. Liu, C. Jiang, G. Liu, Optimal sparse polynomial chaos expansion for arbitrary probability distribution and its application on global sensitivity analysis, Computer Methods in Applied Mechanics and Engineering 399 (2022) 115368.
[8] G. Matheron, The intrinsic random functions and their applications, Advances in Applied Probability 5 (1973) 439–468.
[9] C. K. Williams, C. E. Rasmussen, Gaussian processes for machine learning, volume 2, MIT press Cambridge, MA, 2006.
[10] Y. Pang, Y. Wang, X. Lai, S. Zhang, P. Liang, X. Song, Enhanced Kriging leave-one-out cross-validation in improving model estimation and optimization, Computer Methods in Applied Mechanics and Engineering 414 (2023) 116194.
[11] H. Dai, H. Zhang, W. Wang, G. Xue, Structural reliability assessment by local approximation of limit state functions using adaptive Markov chain simulation and support vector regression, Computer-Aided Civil and Infrastructure Engineering 27 (2012) 676–686.
[12] S. Haoyuan, M. Yizhong, L. Chenglong, Z. Jian, L. Lijun, Hierarchical Bayesian support vector regression with model parameter calibration for reliability modeling and prediction, Reliability Engineering & System Safety 229 (2023) 108842.
[13] T. Zhou, Y. Peng, An active-learning reliability method based on support vector regression and cross validation, Computers & Structures 276 (2023) 106943.
[14] Y. Zhang, J. Xu, Efficient reliability analysis with a CDA-based dimension-reduction model and polynomial chaos expansion, Computer Methods in Applied Mechanics and Engineering 373 (2021) 113467.
[15] I. Papaioannou, M. Ehre, D. Straub, PLS-based adaptation for efficient PCE representation in high dimensions, Journal of Computational Physics 387 (2019) 186–204.

[16] Y. Zhou, Z. Lu, J. Hu, Y. Hu, Surrogate modeling of high-dimensional problems via data-driven polynomial chaos expansions and sparse partial least square, Computer Methods in Applied Mechanics and Engineering 364 (2020) 112906.
[17] B. Echard, N. Gayton, M. Lemaire, N. Relun, A combined importance sampling and kriging reliability method for small failure probabilities with time-demanding numerical models, Reliability Engineering & System Safety 111 (2013) 232–240.
[18] C. Ling, Z. Lu, K. Feng, X. Zhang, A coupled subset simulation and active learning kriging reliability analysis method for rare failure events, Structural and Multidisciplinary Optimization 60 (2019) 2325–2341.
[19] M. Su, G. Xue, D. Wang, Y. Zhang, Y. Zhu, A novel active learning reliability method combining adaptive Kriging and spherical decomposition-MCS (AK-SDMCS) for small failure probabilities, Structural and Multidisciplinary Optimization 62 (2020) 3165–3187.
[20] D. Wang, D. Zhang, Y. Meng, M. Yang, C. Meng, X. Han, Q. Li, AK-HRn: An efficient adaptive Kriging-based n-hypersphere rings method for structural reliability analysis, Computer Methods in Applied Mechanics and Engineering 414 (2023) 116146.
[21] X. Zhang, L. Wang, J. D. Sørensen, REIF: a novel active-learning function toward adaptive Kriging surrogate models for structural reliability analysis, Reliability Engineering & System Safety 185 (2019) 440–454.
[22] C. Peng, C. Chen, T. Guo, W. Xu, AK-SEUR: An adaptive Kriging-based learning function for structural reliability analysis through sample-based expected uncertainty reduction, Structural Safety 106 (2024) 102384.
[23] C. Dang, M. A. Valdebenito, J. Song, P. Wei, M. Beer, Estimation of small failure probabilities by partially Bayesian active learning line sampling: Theory and algorithm, Computer Methods in Applied Mechanics and Engineering 412 (2023) 116068.
[24] Z. Wang, A. Shafieezadeh, ESC: an efficient error-based stopping criterion for kriging-based reliability analysis methods, Structural and Multidisciplinary Optimization 59 (2019) 1621–1637.
[25] J. Wang, G. Xu, Y. Li, A. Kareem, AKSE: a novel adaptive kriging method combining sampling region scheme and error-based stopping criterion for structural reliability analysis, Reliability Engineering & System Safety 219 (2022) 108214.
[26] Y. Zhang, Y. Dong, D. M. Frangopol, An error-based stopping criterion for spherical decomposition-based adaptive Kriging model and rare event estimation, Reliability Engineering & System Safety 241 (2024) 109610.
[27] S. O. Rice, Mathematical analysis of random noise, The Bell System Technical Journal 23 (1944) 282–332.
[28] M. Shinozuka, Simulation of multivariate and multidimensional random processes, The Journal of the Acoustical Society of America 49 (1971) 357–368.
[29] M. Shinozuka, C.-M. Jan, Digital simulation of random processes and its applications, Journal of Sound and Vibration 25 (1972) 111–128.
[30] M. Shinozuka, G. Deodatis, Simulation of stochastic processes by spectral representation (1991).
[31] K.-K. Phoon, H. Huang, S. T. Quek, Simulation of strongly non-Gaussian processes using Karhunen–Loeve expansion, Probabilistic Engineering Mechanics 20 (2005) 188–198.
[32] J.-B. Chen, J. Li, The extreme value distribution and dynamic reliability analysis of nonlinear structures with uncertain parameters, Structural Safety 29 (2007) 77–93.
[33] C. Dang, J. Xu, A mixture distribution with fractional moments for efficient seismic reliability analysis of nonlinear structures, Engineering Structures 208 (2020) 109912.
[34] C. Dang, P. Wei, M. Beer, An approach to evaluation of EVD and small failure probabilities of uncertain nonlinear structures under stochastic seismic excitations, Mechanical Systems and Signal Processing 152 (2021) 107468.
[35] Y. Zhang, Y. Dong, R. Feng, Bayes-informed mixture distribution for the EVD estimation and dynamic reliability analysis, Mechanical Systems and Signal Processing 197 (2023) 110352.
[36] Q. Pan, D. Dias, Sliced inverse regression-based sparse polynomial chaos expansions for reliability analysis in high dimensions, Reliability Engineering & System Safety 167 (2017) 484–493.
[37] T. Zhou, Y. Peng, Structural reliability analysis via dimension reduction, adaptive sampling, and Monte Carlo simulation, Structural and Multidisciplinary Optimization 62 (2020) 2629–2651.
[38] J. Yin, X. Du, Active learning with generalized sliced inverse regression for high-dimensional reliability analysis, Structural Safety 94 (2022) 102151.
[39] T. Zhou, Y. Peng, Efficient reliability analysis based on deep learning-enhanced surrogate modelling and probability density evolution method, Mechanical Systems and Signal Processing 162 (2022) 108064.
[40] B. Schölkopf, A. Smola, K.-R. Müller, Nonlinear component analysis as a kernel eigenvalue problem, Neural computation 10 (1998) 1299–1319.
[41] G. E. Hinton, R. R. Salakhutdinov, Reducing the dimensionality of data with neural networks, science 313 (2006) 504–507.
[42] Y. Peng, T. Zhou, J. Li, Surrogate modeling immersed probability density evolution method for structural reliability analysis in high dimensions, Mechanical Systems and Signal Processing 152 (2021) 107366.
[43] M. Li, Z. Wang, Deep learning for high-dimensional reliability analysis, Mechanical Systems and Signal Processing 139 (2020) 106399.
[44] M. D. Spiridonakos, E. N. Chatzi, Metamodeling of dynamic nonlinear structural systems through polynomial chaos narx models, Computers & Structures 157 (2015) 99–113.
[45] B. Bhattacharyya, E. Jacquelin, D. Brizard, A Kriging–NARX model for uncertainty quantification of nonlinear stochastic dynamical systems in time domain, Journal of Engineering Mechanics 146 (2020) 04020070.
[46] S. Schär, S. Marelli, B. Sudret, Emulating the dynamics of complex systems using autoregressive models on manifolds (mNARX), Mechanical Systems and Signal Processing 208 (2024) 110956.
[47] B. Bhattacharyya, Uncertainty quantification of dynamical systems by a POD–Kriging surrogate model, Journal of Computational Science 60 (2022) 101602.
[48] Y. Yang, P. Perdikaris, Conditional deep surrogate models for stochastic, high-dimensional, and multi-fidelity systems, Computational Mechanics 64 (2019) 417–434.
[49] Z. Wan, J. Chen, W. Tao, P. Wei, M. Beer, Z. Jiang, A feature mapping strategy of metamodelling for nonlinear stochastic dynamical systems with low to high-dimensional input uncertainties, Mechanical Systems and Signal Processing 184 (2023) 109656.
[50] C. Soize, R. Ghanem, Probabilistic-learning-based stochastic surrogate model from small incomplete datasets for nonlinear dynamical systems, Computer Methods in Applied Mechanics and Engineering 418 (2024) 116498.

[51] J. Chen, F. Kong, Y. Peng, A stochastic harmonic function representation for non-stationary stochastic processes, Mechanical Systems and Signal Processing 96 (2017) 31–44.
[52] R. Zhang, Z. Chen, S. Chen, J. Zheng, O. Büyüköztürk, H. Sun, Deep long short-term memory networks for nonlinear structural seismic response prediction, Computers & Structures 220 (2019) 55–68.
[53] R. Zhang, Y. Liu, H. Sun, Physics-informed multi-LSTM networks for metamodeling of nonlinear structures, Computer Methods in Applied Mechanics and Engineering 369 (2020) 113226.
[54] Z. Liu, W. Liu, Y. Peng, Random function based spectral representation of stationary and non-stationary stochastic processes, Probabilistic Engineering Mechanics 45 (2016) 115–126.
[55] X. Huang, J. Chen, H. Zhu, Assessing small failure probabilities by AK–SS: An active learning method combining Kriging and subset simulation, Structural Safety 59 (2016) 86–95.
[56] X. Chen, Z. Lin, Structural nonlinear analysis program OpenSEES theory and tutorial (in Chinese), China Architecture & Building Press, 2020.

Algorithm 2 rLSTM-AE for the low-dimensional latent space detection

Input: Random structural parameters $\mathbf{x}_S$, the stochastic excitation $a(t)$ and observed responses $y(t)$.
Output: rLSTM-AE model and latent variable **Z**.

Data normalization and concatenation:
$\{(\tilde{a}(t), \tilde{\mathbf{x}}_S(t)), \tilde{y}(t)\} \xleftarrow{\text{Eqs.(8)and(9)}} \{a(t), \mathbf{x}_S, y(t)\}$.
$\{\tilde{\mathbf{x}}_{\text{train}}\} \leftarrow \left\{\left(\tilde{a}^i(t), \tilde{\mathbf{x}}_S^i(t)\right)\right\}, \{\tilde{y}_{\text{train}}\} \leftarrow \left\{\tilde{y}^i(t)\right\}, i = 1, 2, ..., N_{\text{train}}$.
$\{\tilde{\mathbf{x}}_{\text{valid}}\} \leftarrow \left\{\left(\tilde{a}^i(t), \tilde{\mathbf{x}}_S^i(t)\right)\right\}, \{\tilde{y}_{\text{valid}}\} \leftarrow \left\{\tilde{y}^i(t)\right\}, i = N_{\text{train}} + 1, N_{\text{train}} + 2, ..., N_{\text{train}} + N_{\text{valid}}$.
rLSTM training:
Specify rLSTM structure: $I_{\text{dim}} = d_2 + 1$,$O_{\text{dim}} = 1$, $l = 2$, $h_s = 50$ and dropout value 0.5.
for m =1:epoch (epoch=500) **do**
  for n=1:batch (samples in each batch $N_{\text{batch}} = 100$) **do**
    $\{\tilde{\mathbf{x}}_{\text{batch}}\}_n \subseteq \{\tilde{\mathbf{x}}_{\text{train}}\}, \{\tilde{y}_{\text{batch}}\}_n \subseteq \{\tilde{y}_{\text{train}}\}; \{\tilde{\mathbf{x}}_{\text{batch}}\}_i \cap \{\tilde{\mathbf{x}}_{\text{batch}}\}_j = \emptyset, i \neq j$.
    $\{\hat{y}_{\text{batch}}\}_n = \text{rLSTM}(\{\tilde{\mathbf{x}}_{\text{batch}}\}_n)$.
    $L_{\text{train}}(\boldsymbol{\lambda}) = \frac{1}{N_{\text{batch}}} \|\{\tilde{y}_{\text{batch}}\}_n - \{\hat{y}_{\text{batch}}\}_n\|_2^2$.
    Backward $L_{\text{train}}(\boldsymbol{\lambda})$ and optimize $\boldsymbol{\lambda}$ with the optimizer "Adam" with a learning rate 0.01.
  end for
  $\{\hat{y}_{\text{valid}}\} = \text{rLSTM}(\{\tilde{\mathbf{x}}_{\text{valid}}\})$.
  $L_{\text{valid}}(m) = \frac{1}{N_{\text{valid}}} \|\{\tilde{y}_{\text{valid}}\} - \{\hat{y}_{\text{valid}}\}\|_2^2$.
end for
Find the minimum validation loss L_{valid} and save the best rLSTM model .
Autoencoder training:
$\{\tilde{y}_{\text{ev,train}}\} = \left\{\tilde{y}_{\text{ev}}^i = \max\left(\text{abs}\left(\tilde{y}^i(t)\right)\right)\right\}, i = 1, 2, ..., N_{\text{train}}$.
$\{\tilde{y}_{\text{ev,valid}}\} = \left\{\tilde{y}_{\text{ev}}^i = \max\left(\text{abs}\left(\tilde{y}^i(t)\right)\right)\right\}, i = N_{\text{train}} + 1, N_{\text{train}} + 2, ..., N_{\text{train}} + N_{\text{valid}}$.
for d_z = 2:20 **do**
  Specify the autoencoder structure: $I_{\text{dim}} = 1$, $O_{\text{dim}} = 1$ and number of nodes in each layer, i.e., ($4d_z$,$2d_z$,d_z) for $E_{\boldsymbol{\varphi}}$ and $(2d_z, 4d_z, O_{\text{dim}})$ for $D_{\boldsymbol{\theta}}$.
  for q=1:epoch (epoch=100) **do**
    for k=1:batch ($N_{\text{batch}} = 100$) **do**
      $\{\tilde{y}_{\text{ev,batch}}\}_k \subseteq \{\tilde{y}_{\text{ev,train}}\}, \{\tilde{y}_{\text{ev,batch}}\}_i \cap \{\tilde{y}_{\text{ev,batch}}\}_j = \emptyset, i \neq j$.
      $\{\hat{y}_{\text{ev,batch}}\}_k = D_{\boldsymbol{\theta}}\left(E_{\boldsymbol{\varphi}}\left(\{\tilde{y}_{\text{ev,batch}}\}_k\right)\right)$.
      $L_{\text{train}}^{\text{AE}}(\boldsymbol{\varphi}, \boldsymbol{\theta}) = \frac{1}{N_{\text{batch}}} \left\|\{\tilde{y}_{\text{ev,batch}}\}_k - \{\hat{y}_{\text{ev,batch}}\}_k\right\|_2^2$.
      Backward $L_{\text{train}}^{\text{AE}}(\boldsymbol{\varphi}, \boldsymbol{\theta})$ and optimize $(\boldsymbol{\varphi}, \boldsymbol{\theta})$ with the optimizer "Adam" with a learning rate 0.01.
    end for
    $\{\hat{y}_{\text{ev,valid}}\} = D_{\boldsymbol{\theta}}(E_{\boldsymbol{\varphi}}(\{\tilde{y}_{\text{ev,valid}}\}))$.
    $L_{\text{valid}}^{\text{AE}}(q) = \frac{1}{N_{\text{batch}}} \|\{\tilde{y}_{\text{ev,valid}}\} - \{\hat{y}_{\text{ev,valid}}\}\|_2^2$.
  end for
  Find the minimum validation loss and save the best autoencoder as $M(d_z)$.
  Obtain latent variables for training GPR: $\mathbf{z}_{\text{train}} \in R^{N_{\text{GPR}} \times d_z} \leftarrow \mathbf{z_0}^{1:N_{\text{GPR}}}, \mathbf{z_0} = E_\varphi(\{\tilde{y}_{\text{ev}}\})$.
  Obtain the original extreme responses for training GPR: $y_{\text{ev,train}} \leftarrow y_{\text{ev}}^{1:N_{\text{GPR}}}, y_{\text{ev}} = \max(\text{abs}(y(t)))$.
  Train GPR and compute error: $L^{\text{GPR}}(d_z) = \frac{1}{N} \sum_{i=1}^{N} \left\|y_{\text{ev}}^i - \text{GPR}\left(\mathbf{z}_0^i\right)\right\|_2^2, N = N_{\text{train}} + N_{\text{valid}}$.
end for
Obtain the best d_z and save the best AE model among $M(d_z)$ by finding the minimum error $L^{\text{GPR}}(d_z)$.
Latent variables detection by the trained rLSTM-AE given unobserved data $a_{\text{new}}(t)$ and $\mathbf{x}_{S,\text{new}}$:
$\{(\tilde{a}_{\text{new}}(t), \tilde{\mathbf{x}}_{S,\text{new}}(t))\} \xleftarrow{\text{Eqs.(8)and(9)}} \{a_{\text{new}}(t), \mathbf{x}_{S,\text{new}}\}$.
$\hat{y}_{\text{new}}(t) = \text{rLSTM}(\{(\tilde{a}_{\text{new}}(t), \tilde{\mathbf{x}}_{S,\text{new}}(t))\}), y_{\text{ev}}^{\text{rLSTM}} = \max(\text{abs}(\hat{y}_{\text{new}}(t)))$.
$\mathbf{z} = E_{\boldsymbol{\varphi}}\left(y_{\text{ev}}^{\text{rLSTM}}\right)$.
Output the rLSTM-AE model and the latent variable **Z**.